This is to certify that the

dissertation entitled

Topics in Plane Elasticity : A Semi-Infinite Bimaterial Strip Under Thermal Loading and A Circular Inclusion in a Half-Plane and An Infinite Strip Under Thermo-Mechanical Loadings

presented by

Mikyoung Lee

has been accepted towards fulfillment
of the requirements for

Ph.D. degree in Mechanics

Irwin Jasiuk
Major professor

Date July 29, 1991

TOPICS IN PLANE ELASTICITY : A SEMI-INFINITE BIMATERIAL STRIP UNDER THERMAL LOADING AND A CIRCULAR INCLUSION IN A HALF-PLANE AND AN INFINITE STRIP UNDER THERMO-MECHANICAL LOADINGS

By

Mikyoung Lee

A DISSERTATION

Submitted to

Michigan State University

in partial fulfillment of the requirements

for the degree of

DOCTOR OF PHILOSOPHY

Department of Metallurgy, Mechanics, and Materials Science

1991

ABSTRACT

Topics in Plane Elasticity : a Semi-Infinite Bimaterial Strip under Thermal Loading and a Circular Inclusion in a Half-Plane and an Infinite Strip under Thermo-Mechanical Loadings

By

Mikyoung Lee

Three problems in plane elasticity are solved exactly in this dissertation. First, the elastic fields due to a circular inclusion embedded in a half-plane subjected either to a uniform uniaxial loading at infinity parallel to the edge boundary, or a uniform non-shear type eigenstrain loading are investigated. The second case is when the inclusion is embedded in an infinite strip. Both the inclusion and the matrix are assumed linear elastic and isotropic. In the above two cases, the interface between the inclusion and the surrounding material is perfectly bonded, or allows pure sliding (shear tractions are specified to vanish). The Papkovich-Neuber displacement potentials in a form of infinite series are used in the analysis. In these problems the joint effect of the free surface (or free surfaces) and interface conditions (perfectly bonded or pure sliding) is studied.

The third problem is of a semi-infinite bimaterial strip that undergoes a constant temperature change. Following Bogy (1968), the Airy stress function method, Mellin transform, and conformal mapping are used to investigate the asymptotic behavior of stresses at the interface near the edge of two strips.

ACKNOWLEDGMENTS

I would like to thank those who have helped in this work. This includes Professor Iwona Jasiuk, who supported me as a friend and as an academic advisor; my guidance committee members: Professor Nicholas Altiero, Professor Robert Soutas-Little, and Professor David Yen, who gave me a chance to complete this work. They are sincerely appreciated.

And Professor E. Tsuchida from Saitama University, Professor T. Mura from Northwestern University and Dr. J. Lau from Hewlett-Packard share my special thanks for their inspiration.

Finally, I want to thank my dad for his encouragement and unlimited support.

Financial support of this work by the National Science Foundation Grant No. MSM-8810920 and the State of Michigan through its 1989-91 Research Excellence Fund is gratefully acknowleged.

TABLE OF CONTENTS

LIST OF FIGURES

NOMENCLATURE

a	-	radius of inclusion
E	-	Young's modulus
G	-	shear modulus
h	-	the width of the strip
K	-	bulk modulus
p_o	-	uniaxial loading
u_i	-	displacement in i-direction
α	-	coefficient of thermal expansion
ϕ_0, ϕ_1	-	Papkovich- Neuber displacement potentials
ϕ	-	Airy stress function
ϵ_{ij}	-	elastic strain tensor
ϵ^*_{ij}	-	inelastic strain tensor
ν	-	Poisson's ratio
σ_{ij}	-	stress tensor
Γ	-	the ratio of shear modulus ($\bar{G}/G$)

CHAPTER 1

INTRODUCTION

Three problems in plane elasticity are solved exactly in this dissertation. First, the problem of a circular inclusion embedded in a half-plane subjected either to a uniform uniaxial loading at infinity parallel to the edge boundary, or a uniform non-shear type eigenstrain loading is investigated. The details are included in Chapter 2. The second case is when the inclusion is embedded in an infinite strip. This solution is discussed in Chapter 3. Both the inclusion and the matrix are assumed linear elastic and isotropic. In the above two cases, the interface between the inclusion and the surrounding material is perfectly bonded, or allows pure sliding (shear tractions are specified to vanish). The Papkovich-Neuber displacement potentials in a form of infinite series are used in the analysis. In the above problems the joint effect of free surface (or free surfaces) and interface conditions (perfectly bonded or pure sliding) is studied. The third problem is of a semi-infinite bimaterial strip that undergoes a constant temperature change. The solution is given in Chapter 4. Following Bogy (1968), the Airy stress function method, Mellin transform, and conformal mapping are used to investigate the asymptotic behavior of stresses at the interface near the edge of two strips.

The presence of inhomogeneities (inclusions) in an elastic material has been the subject of extensive investigations due to the importance of stress concentrations in the design. When inclusions exist in a material, the stress is intensified in their vicinity. The degree of this stress disturbance depends on the mismatch of the elastic

constants, the shape, the size, the location of the inclusions, the boundary conditions at the inclusion-matrix interface, the loading, and other factors.

As a literature background most of the papers dealing with inclusions (see Mura, 1987), along with Eshelby's celebrated paper (Eshelby, 1957), involve the cases when the inclusion is embedded in an infinitely extended material and is perfectly bonded.

The two dimensional problem of a semi-infinite plate with a hole subjected to a uniaxial loading was solved by Jeffery (1920). Jeffery's paper, however, contains an error and the solution does not satisfy the traction free boundary conditions at the straight edge. The above solution was corrected by Mindlin (1948). This problem has been reexamined recently by Callias and Markenskoff (1989), who analyzed the singularity of the hoop stress at a hole, as the hole approaches the free boundary. The problem of a circular inclusion in a half-plane undergoing an expansion was solved by Richardson (1969). The inclusion was assumed to be of the same material as the matrix. The problem of a semi-infinitely extended material with a perfectly bonded circular inclusion was addressed by Saleme (1958). Coincidentally, Saleme's solution also contains an error, since it does not include the rigid body displacement of the inclusion, as pointed out by Shioya (1967). Most of the above authors used bipolar coordinates and Airy stress functions in a form of infinite series in their analysis.

The problem of an infinite strip with a hole under a uniaxial tension loading was solved by Howland (1929). In his paper a solution was sought by the successive approximation method. Later, Howland and Stevenson (1933) considered a more general problem which includes unsymmetrical cases. Wang (1946) studied perforated shear webs. He

considered an infinitely long plate of a finite width with a plain circular hole and rectangular plate with a plain or reinforced circular hole. The problem of determining the stresses in a perforated strip loaded in tension through a close-fitting rigid pin filling the hole was solved by Theocaris (1954). In his paper, there are some limitations like that the inclusion, which represents a pin, is rigid and the ratio of the diameter of the hole and the breadth of the strip does not exceed 0.5. The analytical solution of an infinite strip having an unsymmetically located perforating hole was investigated by Ling (1956). This can be considered as a complete solution because it is valid in the entire strip, unlike the previous solution by Howland and Stevenson (1933) for a symmetrically perforated strip. Tamate (1956) studied the effect of a circular hole in an infinite strip subjected to a pure twist by using the perturbation method.

The problem of a sliding inclusion in an infinite material was addressed in two dimensions by Tsuchida et al. (1986) and Kouris et al. (1988), and in three dimensions by Mura and Furuhashi (1984), Mura et al. (1985), and Jasiuk et al. (1987). The problem of a sliding hemi-spherical or hemi-spheroidal inclusion at a free surface was solved by Kouris and Mura (1989), Kouris et al. (1989), and Tsuchida et al. (1990).

The half-plane problem in three dimensions for eigenstrain loading was solved by Mindlin and Cheng (1950) and Aderogba (1976) for a spherical inclusion, and by Seo and Mura (1979) for an ellipsoidal inclusion. The problem of an inhomogeneity near the free surface subjected to all-around tension at infinity was solved by Tsutsui and Saito (1973) for a spherical inclusion and Tsuchida and Mura (1983) for a spheroidal inclusion.

The three dimensional problems of an infinite strip with a prolate spheroidal cavity subjected to an axisymmetric pressure and a uniaxial tension were investigated by Tsuchida and Yaegashi (1981a, 1981b). The solution of this problem is based upon Boussinesq's stress function approach.

In this dissertation we consider a problem of a sliding circular inclusion embedded in a half-plane or a semi-infinite strip. We are interested in the joint effect of the free surface and sliding boundary condition. This problem has not been addressed before.

When two different materials are bonded together and subjected to a temperature change, the thermal stress will arise due to the different thermal expansion coefficients.

A number of studies on bimaterial strips subjected to temperature change are reported in literature. The first solution, based on beam theory, was given by Timoshenko (1925). The problem of edge effects was first addressed by Aleck (1949). The more recent solutions include approximate solutions (Hess, 1969; Chen and Nelson, 1979; Chen et al., 1982; Blech and Kantor, 1984; Suhir, 1986, 1989; Gerstle and Chambers, 1987) and elasticity solution of Kuo (1989), to mention some. The finite element solutions of this problem are discussed by Lau (1989). Additional references are given in Eischen et al. (1990). The solutions to the related problems include the bimaterial subjected to mechanical loading (Bogy, 1968; Hess, 1969). Also, the singularity of the interfacial stresses at the edge is discussed by Bogy (1970), and Blanchard and Ghoniem (1989) for the case of bonded dissimilar quarter planes, and by Hein and Erdogan (1971), and Dempsey and Sinclair (1981) for the case of the bimaterial wedges. For the above mentioned geometries the singularity is shown to depend on the elastic constants.

In this dissertation we consider a problem of a bimaterial semi-infinite strip. This problem was studied before as mentioned above. But the existing results are approximate, using either strength of materials approach or finite element method. Here we solve this problem exactly by using theory of elasticity. We find that stresses are singular at the interface at the edge of the strip.

CHAPTER 2 : A Circular Inclusion in A Half-Plane

INTRODUCTION

In this part of dissertation, the plane elasticity problem of a circular inclusion embedded in a half-plane is considered. The solution will apply to two physical cases of a disk-like inclusion embedded in a semi-infinite plate (plane stress), or a cylindrical inclusion embedded in a half-space (plane strain). The inclusion has different elastic constants from those of the matrix. The inclusion may represent the cross-section of a fiber located near the free surface of a composite material. The loading is either a uniaxial stress at infinity parallel to the edge boundary, or a uniform non-shear type eigenstrain (transformation strain) given by ϵ^*_{ij}, such that i = j, where i,j = x,y,z. Both the inclusion and the surrounding matrix are assumed to be linear elastic and isotropic. The interface between the inclusion and the matrix allows sliding: the shear tractions are specified to vanish and no separation takes place in the normal direction. The perfect bonding case is included for comparison. In this study the joint effect of a traction free edge boundary and sliding is investigated.

METHOD OF SOLUTION

Consider a semi-infinite material having a circular inclusion subjected to a uniaxial loading or uniform eigenstrains. Let the origin of coordinates be at the center of the circular inclusion and the x-axis be directed down into the interior of the semi-infinite body. It is

convenient to use a polar coordinate system, which is related to the Cartesian system by $x = r\cos\theta$ and $y = r\sin\theta$. Without loss of generality, the distance between the center of inclusion and the point on the free boundary closest to the inclusion is taken as unity. Therefore, the free surface (the straight edge of the plate or the plane surface of the semi-infinite body) is given by $x = -1$. The radius of inclusion is taken as $r = a$.

The following boundary conditions are used:

i) the traction free condition on the surface $x = -1$:

$$(\sigma_{xx})_{x=-1} = (\sigma_{xy})_{x=-1} = 0 \tag{2.1}$$

ii) either the pure sliding conditions at the interface of the inclusion:

$$\begin{aligned} &(\sigma_{rr})_{r=a} = (\bar{\sigma}_{rr})_{r=a} \\ &(\sigma_{r\theta})_{r=a} = (\bar{\sigma}_{r\theta})_{r=a} = 0 \\ &(u_r)_{r=a} = (\bar{u}_r)_{r=a} \end{aligned} \tag{2.2}$$

or the perfect bonding conditions at the interface of the inclusion:

$$\begin{aligned} &(\sigma_{rr})_{r=a} = (\bar{\sigma}_{rr})_{r=a} \\ &(\sigma_{r\theta})_{r=a} = (\bar{\sigma}_{r\theta})_{r=a} \\ &(u_r)_{r=a} = (\bar{u}_r)_{r=a} \end{aligned} \tag{2.3}$$

$$(u_\theta)_{r=a} = (\bar{u}_\theta)_{r=a}$$

iii) either a uniaxial stress applied at infinity:

$$\sigma_{xx} = 0, \qquad \sigma_{xy} = 0, \qquad \sigma_{yy} = p_o \tag{2.4}$$

or the vanishing tractions for eigenstrain case:

$$\sigma_{ij} = 0, \qquad i,j = x,y. \tag{2.5}$$

In the preceding expressions the quantities defined in the inclusion are denoted by a superior bar.

The Papkovich-Neuber displacement potentials are used to solve the above boundary value problems. The displacement potentials, ϕ_0 and ϕ_1, that account for the disturbance due to the inhomogeneity and the effect of free surface, are given as follows:

i) for the matrix ($r > a$), ϕ_0 and ϕ_1 are

(I)
$$\begin{cases} \phi_0 = C_0 \left(-A_0 \log r + \sum_{m=1}^{\infty} A_m \dfrac{\cos m\theta}{r^m} \right) \\ \phi_1 = C_0 \sum_{m=0}^{\infty} B_m \dfrac{\cos m\theta}{r^m} \end{cases} \tag{2.6}$$

(II)
$$\begin{cases} \phi_0 = C_0 \displaystyle\int_0^{\infty} \psi_1(\lambda)\, e^{-\lambda x} \cos \lambda y \, d\lambda \\ \phi_1 = C_0 \displaystyle\int_0^{\infty} \lambda\, \psi_2(\lambda)\, e^{-\lambda x} \cos \lambda y \, d\lambda \end{cases} \tag{2.7}$$

ii) and for the inclusion ($r < a$), ϕ_0 and ϕ_1 are

$$\text{(III)} \qquad \begin{cases} \phi_0 = C_0 \sum_{n=0}^{\infty} \bar{A}_n \, r^n \cos n\theta \\ \phi_1 = C_0 \sum_{n=0}^{\infty} \bar{B}_n \, r^n \cos n\theta \end{cases} \tag{2.8}$$

where

$$C_0 = \begin{cases} p_o & \text{for a uniaxial loading} \\ 2G\epsilon^* & \text{for an eigenstrain loading } (\epsilon^* = \epsilon^*_{xx}, \ \epsilon^*_{yy} \text{ or } \epsilon^*_{zz}) \end{cases}$$

where G is the shear modulus of the matrix and ϵ^*_{xx}, ϵ^*_{yy} and ϵ^*_{zz} are the eigenstrains. A_m, B_m, $\bar{A}_n$ and $\bar{B}_n$ are the unknown constants and $\psi_1(\lambda)$ and $\psi_2(\lambda)$ are the unknown functions of λ, which are determined from the boundary conditions (2.1)-(2.5). Note that (I) is expressed by a suffix m and (III) by a suffix n. For reference, the relations between the displacement potentials ϕ_0 and ϕ_1 and the stresses and displacements are given in the Appendix.

When a uniaxial loading is applied, the displacement potentials are given as

$$\text{(IV)} \qquad \begin{cases} \phi_0 = \dfrac{p_o}{8} (\kappa+1)(y^2 - x^2) \\ \phi_1 = -\dfrac{p_o}{2} x. \end{cases} \tag{2.9}$$

The stresses and displacements obtained from (IV) are given as

$$\sigma_{xx} = 0$$

$$\sigma_{xy} = 0$$

$$\sigma_{yy} = p_o \tag{2.10}$$

$$2G\, u_x = -\frac{3-\kappa}{4}\, p_o\, x$$

$$2G\, u_y = \frac{\kappa+1}{4}\, p_o\, y$$

where

$$\kappa = \begin{cases} 3 - 4\nu & \text{for plane strain} \\ \dfrac{3 - \nu}{1 + \nu} & \text{for plane stress} \end{cases}$$

where ν is Poisson's ratio. The stresses and displacements, given in equation (2.10), are expressed in polar coordinates as

$$\sigma_{rr} = p_o \frac{1}{2} (1 - \cos 2\theta)$$

$$\sigma_{r\theta} = p_o \frac{1}{2} \sin 2\theta$$

$$\sigma_{\theta\theta} = p_o \frac{1}{2} (1 + \cos 2\theta) \tag{2.11}$$

$$2G\, u_r = p_o \frac{r}{4} \{(\kappa-1) - 2\cos 2\theta\}$$

$$2G\, u_\theta = p_o \frac{r}{2} \sin 2\theta.$$

When the inclusion is subjected to an eigenstrain loading, the displacements inside the inhomogeneity are the sum of displacements of the inclusion if there would be no constraint from the matrix

$$u_x^* = (\epsilon_{xx}^* + \eta\, \epsilon_{zz}^*)\, x$$

$$u_y^* = (\epsilon_{yy}^* + \eta\, \epsilon_{zz}^*)\, y \qquad (2.12)$$

where

$$\eta = \begin{cases} \nu & \text{for plane strain} \\ 0 & \text{for plane stress} \end{cases}$$

and the elastic displacements obtained from (III). The displacements, given in (2.12) are expressed in polar coordinates as

$$u_r^* = \frac{r}{2} \{ 2\eta\, \epsilon_{zz}^* + (\epsilon_{xx}^* + \epsilon_{yy}^*) + (\epsilon_{xx}^* - \epsilon_{yy}^*) \cos 2\theta \}$$

$$u_\theta^* = \frac{r}{2} (\epsilon_{yy}^* - \epsilon_{xx}^*) \sin 2\theta. \qquad (2.13)$$

The corresponding stresses are zero.

Note, that the stress components derived from (I) and (II) vanish at infinity. Therefore, for the eigenstrain loading the boundary condition (2.5) is automatically satisfied. For the case of uniaxial loading, ϕ_0 and ϕ_1, given by (IV), yield the uniaxial tension p_o. Therefore, the boundary condition (2.4) is also automatically satisfied. To satisfy the traction free boundary condition (2.1) at the free surface, (I) is considered as follows:

(I)-1 $\qquad \phi_0 = - C_0 A_0 \log r$

$$\text{(I)-2} \qquad \begin{cases} \phi_0 = C_0 \sum_{m=1}^{\infty} A_m \dfrac{\cos m\theta}{r^m} \\ \phi_1 = C_0 \sum_{m=0}^{\infty} B_m \dfrac{\cos m\theta}{r^m} . \end{cases} \tag{2.14}$$

Using one of the following mathematical relations

$$\frac{\cos m\theta}{r^m} = \frac{(-1)^m}{(m-1)!} \int_0^{\infty} \lambda^{m-1} e^{\lambda x} \cos \lambda y \, d\lambda$$

$$\frac{\sin m\theta}{r^m} = \frac{(-1)^{m-1}}{(m-1)!} \int_0^{\infty} \lambda^{m-1} e^{\lambda x} \sin \lambda y \, d\lambda, \qquad (x < 0) \tag{2.15}$$

(I)-2 is expressed in Cartesian coordinates as

$$\text{(I)-2}^* \qquad \begin{cases} \phi_0 = C_0 \sum_{m=1}^{\infty} \dfrac{(-1)^m}{(m-1)!} A_m \displaystyle\int_0^{\infty} \lambda^{m-1} e^{\lambda x} \cos \lambda y \, d\lambda & (x < 0) \\ \phi_1 = C_0 \sum_{m=1}^{\infty} \dfrac{(-1)^m}{(m-1)!} B_m \displaystyle\int_0^{\infty} \lambda^{m-1} e^{\lambda x} \cos \lambda y \, d\lambda. & (2.16) \end{cases}$$

As for (I)-1,

$$\phi_0 = -C_0 A_0 \log r = - C_0 A_0 \frac{1}{2} \log (x^2 + y^2) \tag{2.17}$$

and the stresses are obtained directly from equation (2.17) as

$$\sigma_{xx} = C_0 A_0 \frac{\cos 2\theta}{r^2}$$

$$\sigma_{xy} = C_0 A_0 \frac{\sin 2\theta}{r^2} \tag{2.18}$$

and using (2.15) they are expressed as

$$\sigma_{xx} = C_0 A_0 \int_0^\infty \lambda e^{\lambda x} \cos \lambda y \, d\lambda$$

$$(x < 0) \tag{2.19}$$

$$\sigma_{xy} = - C_0 A_0 \int_0^\infty \lambda e^{\lambda x} \sin \lambda y \, d\lambda.$$

Using equations (2.7), (2.16) and (2.19), the boundary conditions (2.1) are written as

$$\left(\frac{\sigma_{xx}}{C_0}\right)_{x=-1} = \int_0^\infty \lambda^2 [\psi_1(\lambda) e^{\lambda} + (\frac{\kappa+1}{2} - \lambda) \psi_2(\lambda) e^{\lambda} + \sum_{m=1}^{\infty} A_m \frac{(-1)^m}{(m-1)!} \lambda^{m-1} e^{-\lambda}$$

$$- \sum_{m=1}^{\infty} (\frac{\kappa+1}{2} + \lambda) \lambda^{m-2} e^{-\lambda} B_m \frac{(-1)^m}{(m-1)!} + A_0 \lambda^{-1} e^{-\lambda}] \cos \lambda y \, d\lambda = 0 \tag{2.20}$$

$$\left(\frac{\sigma_{xy}}{C_0}\right)_{x=-1} = \int_0^\infty \lambda^2 [\psi_1(\lambda) e^{\lambda} + (\frac{\kappa-1}{2} - \lambda) \psi_2(\lambda) e^{\lambda} - \sum_{m=1}^{\infty} A_m \frac{(-1)^m}{(m-1)!} \lambda^{m-1} e^{-\lambda}$$

$$+ \sum_{m=1}^{\infty} (\frac{\kappa-1}{2} + \lambda) \lambda^{m-2} e^{-\lambda} \frac{B_m (-1)^m}{(m-1)!} - A_0 \lambda^{-1} e^{-\lambda}] \sin \lambda y \, d\lambda = 0. \tag{2.21}$$

Setting the quantities in the brackets in equations (2.20)-(2.21) to zero, two equations for the two unknowns $\psi_1(\lambda)$ and $\psi_2(\lambda)$ are obtained. Solving these equations, $\psi_1(\lambda)$ and $\psi_2(\lambda)$ are found as

$$\psi_1(\lambda) = A_0 \lambda^{-1} e^{-2\lambda} (\kappa-2\lambda) + \sum_{m=1}^{\infty} \left[\frac{A_m(-1)^m}{(m-1)!} \lambda^{m-1} e^{-2\lambda}(\kappa-2\lambda) \right.$$

$$\left. - B_m \frac{(-1)^m}{(m-1)!} \lambda^{m-2} e^{-2\lambda} \frac{(\kappa^2 - 1 - 4\lambda^2)}{2} \right] \tag{2.22}$$

$$\psi_2(\lambda) = -2A_0 \lambda^{-1} e^{-2\lambda} - \sum_{m=1}^{\infty} \left[2 \frac{A_m(-1)^m}{(m-1)!} \lambda^{m-1} e^{-2\lambda} \right.$$

$$\left. - \frac{B_m(-1)^m}{(m-1)!} (\kappa+2\lambda) \lambda^{m-2} e^{-2\lambda} \right]. \tag{2.23}$$

In order to satisfy the boundary conditions (2.2) or (2.3) at the inclusion's interface, the following relation is used

$$e^{-\lambda x} \cos \lambda y = \sum_{n=0}^{\infty} (-1)^n \frac{(\lambda r)^n}{n!} \cos n\theta. \tag{2.24}$$

(II) is rewritten by using equation (2.24) as follows

$$(II)^* \quad \begin{cases} \phi_0 = C_0 \sum_{n=0}^{\infty} \alpha_n r^n \cos n\theta \\ \phi_1 = C_0 \sum_{n=0}^{\infty} \beta_n r^n \cos n\theta \end{cases} \tag{2.25}$$

where

$$\alpha_n = \int_0^{\infty} \psi_1(\lambda) \frac{(-1)^n \lambda^n}{n!} d\lambda \tag{2.26}$$

$$\beta_n = \int_0^\infty \lambda\, \psi_2(\lambda)\, \frac{(-1)^n \lambda^n}{n!}\, d\lambda$$

and

$$\alpha_n = A_0\, \alpha_{n1} + \sum_{m=1}^{\infty} \alpha_{n2}^m\, A_m + \sum_{m=1}^{\infty} \alpha_{n3}^m\, B_m$$

$$\beta_n = A_0\, \beta_{n1} + \sum_{m=1}^{\infty} \beta_{n2}^m\, A_m + \sum_{m=1}^{\infty} \beta_{n3}^m\, B_m \qquad (2.27)$$

where

$$\alpha_{n1} = \int_0^\infty (\kappa - 2\lambda)\, (-1)^n\, \frac{\lambda^{n-1}}{n!}\, e^{-2\lambda}\, d\lambda$$

$$\alpha_{n2}^m = \int_0^\infty (\kappa - 2\lambda)\, (-1)^{m+n}\, \frac{\lambda^{m+n-1}}{(m-1)!\; n!}\, e^{-2\lambda}\, d\lambda$$

$$\alpha_{n3}^m = \int_0^\infty \frac{(\kappa^2 - 1 - 4\lambda^2)}{2}\, (-1)^{m+n+1}\, \frac{\lambda^{m+n-2}}{(m-1)!\; n!}\, e^{-2\lambda}\, d\lambda$$

$$\beta_{n1} = \int_0^\infty (-2)\, (-1)^n\, \frac{\lambda^n}{n!}\, e^{-2\lambda}\, d\lambda \qquad (2.28)$$

$$\beta_{n2}^m = \int_0^\infty (-2)\, (-1)^{m+n}\, \frac{\lambda^{m+n}}{(m-1)!\; n!}\, e^{-2\lambda}\, d\lambda$$

$$\beta_{n3}^m = \int_0^\infty (\kappa + 2\lambda)\, (-1)^{n+m}\, \frac{\lambda^{m+n-1}}{(m-1)!\; n!}\, e^{-2\lambda}\, d\lambda.$$

Using Euler's Integral of second kind

$$\int_0^\infty e^{-ax} x^b \, dx = \frac{\Gamma(b+1)}{a^{b+1}} \qquad (a, b > 0) \qquad (2.29)$$

and the relation

$$\int_0^\infty \frac{1}{\xi} e^{-\xi z} \cos \xi a \, d\xi = -\frac{1}{2} \log (a^2 + z^2) \qquad (2.30)$$

equations (2.28) can be simplified as

$$\alpha_{n1} = -\kappa \epsilon_n - 2 \gamma_n^0$$

$$\alpha_{n2}^m = -\kappa \gamma_n^{m-1} - 2m \gamma_n^m$$

$$\alpha_{n3}^m = \frac{\kappa^2 - 1}{2} \gamma_n^{m-1} - 2m (m+1) \gamma_n^m \qquad (2.31)$$

$$\beta_{n1} = -2 \gamma_n^0$$

$$\beta_{n2}^m = -2m \gamma_n^m$$

$$\beta_{n3}^m = m \kappa \gamma_n^m - 2m (m+1) \gamma_n^m$$

where

$$\gamma_n^m = \frac{(-1)^{m+n}}{m! \, n!} \int_0^\infty e^{-2\lambda} \lambda^{m+n} \, d\lambda = \frac{(-1)^{m+n}}{m! \, n!} \frac{(m+n)!}{2^{m+n+1}} \qquad (2.32)$$

and

$$\epsilon_n = \begin{cases} \log 2 & n = 0 \\ 0 & \\ \dfrac{\gamma_{n-1}}{n} & n \geq 1 \end{cases} \tag{2.33}$$

Next, the stresses and displacements are derived from the displacement potentials given by (I), (II)* and (III), and the equations (2.11) are used for a uniaxial loading and equations (2.13) for eigenstrain loading cases. Substituting these results in the sliding boundary conditions (2.2), the following four equations are obtained:

i) the continuity of normal tractions $(\sigma_{rr})_{r=a} = (\bar{\sigma}_{rr})_{r=a}$:

$$\sum_{n=0}^{\infty} [s_{A1} A_n + s_{B1} B_{n-1} + s_{B2} B_{n+1} + s_{\alpha 1} \alpha_n + s_{\beta 1} \beta_{n-1} + s_{\beta 2} \beta_{n+1}$$

$$- \bar{s}_{A1} \bar{A}_n - \bar{s}_{B1} \bar{B}_{n-1} - \bar{s}_{B2} \bar{B}_{n+1}] \cos n\theta = \frac{A_0}{a^2} - \frac{p_o}{C_0} \frac{(1-\cos 2\theta)}{2} \tag{2.34}$$

ii) the condition of continuity of normal displacements $(u_r)_{r=a} = (\bar{u}_r)_{r=a}$:

$$\sum_{n=0}^{\infty} [\{k_{A1} A_n + k_{B1} B_{n-1} + k_{B2} B_{n+1} + k_{\alpha 1} \alpha_n + k_{\beta 1} \beta_{n-1} + k_{\beta 2} \beta_{n+1}\}$$

$$- \frac{1}{\Gamma} \{\bar{k}_{A1} \bar{A}_n + \bar{k}_{B1} \bar{B}_{n-1} + \bar{k}_{B2} \bar{B}_{n+1}\}] \cos n\theta =$$

$$\frac{A_0}{a} - \frac{p_o}{C_0} \frac{a}{4} \{ (1-\kappa) - 2 \cos 2\theta \} +$$

$$\frac{2G}{C_0} \frac{a}{2} \{ 2\eta \epsilon^*_{zz} + (\epsilon^*_{xx} + \epsilon^*_{yy}) + (\epsilon^*_{xx} - \epsilon^*_{yy}) \cos 2\theta \} \tag{2.35}$$

iii) the continuity of tangential tractions $(\sigma_{r\theta})_{r=a} = (\bar{\sigma}_{r\theta})_{r=a}$:

$$\sum_{n=1}^{\infty} [t_{A1} A_n + t_{B1} B_{n-1} + t_{B2} B_{n+1} + t_{\alpha 1}\alpha_n + t_{\beta 1} \beta_{n-1} + t_{\beta 2} \beta_{n+1}$$

$$- \bar{t}_{A1} \bar{A}_n - \bar{t}_{B1} \bar{B}_{n-1} - \bar{t}_{B2} \bar{B}_{n+1}] \sin n\theta = - \frac{p_o}{c_0} \frac{1}{2} \sin 2\theta \qquad (2.36)$$

iv) and the condition of vanishing shear tractions given by either $(\bar{\sigma}_{r\theta})_{r=a} = 0$:

$$\sum_{n=1}^{\infty} [\bar{t}_{A1} \bar{A}_n + \bar{t}_{B1} \bar{B}_{n-1} + \bar{t}_{B2} \bar{B}_{n+1}] \sin n\theta = 0 \qquad (2.37)$$

or $(\sigma_{r\theta})_{r=a} = 0$.

The problem of the perfectly bonded inclusion can be solved by using the first three equations, (2.34)-(2.36), and the last one, (2.37), is replaced by the condition of continuity of tangential displacements $(u_\theta)_{r=a} = (\bar{u}_\theta)_{r=a}$:

$$\sum_{n=1}^{\infty} [\{ l_{A1} A_n + l_{B1} B_{n-1} + l_{B2} B_{n+1} + l_{\alpha 1} \alpha_n + l_{\beta 1} \beta_{n-1} + l_{\beta 2}$$

$$\beta_{n+1}\} - \frac{1}{\Gamma} \{ \bar{l}_{A1} \bar{A}_n + \bar{l}_{B1} \bar{B}_{n-1} + \bar{l}_{B2} \bar{B}_{n+1} \}] \sin n\theta = - \frac{p_o}{c_0} \frac{a}{2} \sin 2\theta$$

$$+ \frac{2G}{c_0} \frac{a}{2} (\epsilon^*_{yy} - \epsilon^*_{xx}) \sin 2\theta \qquad (2.38)$$

where $\Gamma = \bar{G} / G$, and G and $\bar{G}$ are the shear moduli of the matrix and inclusion, respectively, and

$$k_{A1} = \frac{-n}{a^{n+1}}, \qquad k_{B1} = \frac{-(n-1+\kappa)}{2a^{n-1}}, \qquad k_{B2} = \frac{-(n+1+\kappa)}{2a^{n+1}},$$

$$k_{\alpha 1} = na^{n-1}, \qquad k_{\beta 1} = \frac{(n-1-\kappa)a^{n-1}}{2}, \qquad k_{\beta 2} = \frac{(n+1-\kappa)a^{n+1}}{2} \tag{2.39}$$

$$l_{A1} = \frac{-n}{a^{n+1}}, \qquad l_{B1} = \frac{-(n-1-\kappa)}{2a^{n-1}}, \qquad l_{B2} = \frac{-(n+1+\kappa)}{2a^{n+1}},$$

$$l_{\alpha 1} = (-n)\, a^{n-1}, \qquad l_{\beta 1} = \frac{(\kappa-n+1)a^{n-1}}{2}, \qquad l_{\beta 2} = \frac{-(\kappa+n+1)a^{n+1}}{2} \tag{2.40}$$

$$s_{A1} = \frac{n(n+1)}{a^{n+2}}, \qquad s_{B1} = \frac{(n-1)(n+2)}{2a^{n}}, \qquad s_{B2} = \frac{(n+1)(n+1+\kappa)}{2a^{n+2}},$$

$$s_{\alpha 1} = n(n-1)a^{n-2}, \qquad s_{\beta 1} = \frac{(n-1)(n-1-\kappa)\, a^{n-2}}{2}, \qquad s_{\beta 2} = \frac{(n+1)(n-2)a^{n}}{2} \tag{2.41}$$

$$t_{A1} = \frac{n(n+1)}{a^{n+2}}, \qquad t_{B1} = \frac{n(n-1)}{2a^{n}}, \qquad t_{B2} = \frac{(n+1)(n+1+\kappa)}{2a^{n+2}}$$

$$t_{\alpha 1} = (-n)(n-1)a^{n-2}, \qquad t_{\beta 1} = \frac{(1-n)(n-1-\kappa)\, a^{n-2}}{2}, \qquad t_{\beta 2} = \frac{-(1+n)n\, a^{n}}{2} \tag{2.42}$$

Note that the terms involving barred quantities $\bar{k}_{A1}$, $\bar{k}_{B1}$, $\bar{l}_{A1}$, ... can be obtained directly from $k_{\alpha 1}$, $k_{\beta 1}$, $l_{\alpha 1}$, ... by replacing κ with $\bar{\kappa}$.

The displacement containing the coefficients α_1 and β_0 corresponds to the rigid body motion of the matrix. Therefore, α_1 and β_0 are taken

as zero. The displacements containing $\bar{A}_1$ and $\bar{B}_0$ represent the rigid body motion of the inclusion in x-direction. Since the terms containing $\bar{A}_1$ and $\bar{B}_0$ give the same rigid body displacement of the inclusion, one of the two constants can be chosen to be zero. In this paper, $\bar{B}_0 = 0$ and $\bar{A}_1 \neq 0$ ($\bar{B}_0 \neq 0$, $\bar{A}_1 = 0$ will give the same result).

Equating the coefficients of sin $n\theta$ and cos $n\theta$ in the left and right sides of either equations (2.34)-(2.37) for the sliding case, or (2.34)-(2.36) and (2.38) for the perfect bonding case, an infinite set of algebraic equations for the unknown constants A_n, B_n, $\bar{A}_n$ and $\bar{B}_n$ is obtained. Each of these four sets of unknowns is associated with an integer n, which varies from zero or one to infinity. In the numerical calculations the infinite series are truncated at $n = N$. For the examples included in this paper N ranges from 2 to 33. N is chosen in such a way that the boundary conditions are satisfied to 3 or more significant figures, which means that the error involved is 1.0×10^{-3}% or less. The accuracy is improved by increasing a number of terms in the series. The solution holds for the whole range of a, $0 < a < 1$. As $a \to 1$, only the number of terms needs to be increased. When a perfectly bonded or sliding inclusion is embedded in the infinite matrix, i.e. the inclusion is far away from the free surface, the solution is given by finite series involving n=0 and n=2. After A_n, B_n, $\bar{A}_n$ and $\bar{B}_n$ are evaluated the stresses and displacements are known everywhere in the inclusion and the matrix.

RESULTS AND DISCUSSION

In the numerical examples considered in this Chapter the plane strain case is assumed. This case is of interest in the light of

applications to composite materials reinforced with unidirectional fibers. For simplicity $\nu = \bar{\nu} = 0.3$ is taken.

Figs. 2-3 illustrate the stress σ_{yy} at points M, N, N', P, and P' (see Fig. 1) for perfect bonding (dashed lines) and pure sliding (solid lines) cases for different positions of the inclusion relative to the free surface. The radius "a" is varied from 0.2 to 0.99, while the center of the inclusion remains at a unit distance from the free surface (Fig. 1). The loading conditions include the remote uniaxial stress $\sigma_{yy} = p_o$ (Fig. 2) and the eigenstrain loading $\epsilon^*_{xx} = \epsilon^*_{yy} = \epsilon^*_{zz}$ (Fig. 3). The inclusion is assumed to be stiffer than the matrix such that the ratio $\Gamma = \bar{G}/G = 100$ (note that the higher the Γ, the more pronounced the effect of interface). It can be observed that the effect of free surface contributes significantly to the stress disturbance when the inclusion is embedded less than one diameter away from the free surface (which corresponds to $1/a < 3$).

When the uniaxial loading is applied (Fig. 2) and the inhomogeneity is perfectly bonded, the maximum stress σ_{yy} occurs in the inclusion at the point N', which is closest to the free surface. The stress in the matrix near the inclusion is almost zero since the inclusion, which is stiffer than the matrix, carries the load. It is also observed that the stress σ_{yy} at the free surface is less than the applied load when the inclusion is close to the free surface.

Quite a different behavior is observed when the sliding takes place at the interface. The highest stress occurs in the matrix near the free surface when the inclusion is close to the free boundary. It is interesting to observe that the hoop stress in the sliding inclusion at points N' and P' and the vicinity is compressive, while the perfect bonding solution yields tensile stresses in these regions. This compressive stress in the sliding inclusion is due to the fact that the

sliding interface does not transfer shear tractions and due to the curvature of the inclusion. Therefore, the matrix, which is allowed to flow more freely around the inclusion causes the local compressive stress in the inclusion.

When the inclusion is soft ($\Gamma \ll 1$), the presence of the free surface gives rise to a very high stress concentration in the matrix at point N. For this case the contribution of interface is negligible. This is expected, because in a limiting case when the inclusion becomes a hole ($\Gamma = 0$), both perfect bonding and sliding cases reduce to the same result. In this limit case the present solution (for plane stress case) coincides with Mindlin's solution (Mindlin, 1948). When inclusion is away from the free surface, the solution agrees with the result for the inclusion embedded in the infinitely extended material (Muskhelishvili, 1953; Eshelby, 1957), as expected.

When discussing the solution of a sliding inclusion, which is subjected to either a uniaxial remote loading or an eigenstrain loading (non-dilatational), a comment needs to be made about the tensile normal tractions that may arise at the inclusion-matrix interface. These tensile tractions imply a tendency to debond in the normal direction, but the debonding is not allowed by the sliding boundary conditions. In order to avoid the possibility of debonding, the case of remote loading may be considered in conjunction with the eigenstrain loading, when the eigenstrains are chosen in a way that the total radial stress is compressive all along the interface as suggested by Muskhelishvili (1953). This case can be obtained by a superposition of these two solutions. However, it is more informative to separate these two cases when giving the numerical results. The more realistic boundary conditions for this problem would allow for a local debonding. This would give rise to a mixed boundary value problem. The analytical

solutions to a problem, when a sliding inclusion is subjected to a uniaxial tensile loading at infinity and debonding is allowed are given by Stippes et al. (1962), Noble and Hussain (1969), Margetson and Morland (1970), and Keer et al. (1973), among others. In this dissertation, the debonding in the normal direction is not allowed, for simplicity.

Fig. 3 illustrates σ_{yy} at chosen points along the x axis for eigenstrain loading $\epsilon^*_{xx} = \epsilon^*_{yy} = \epsilon^*_{zz}$ for both perfect bonding and pure sliding. The highest stress occurs in the matrix at the free surface for the sliding case. Also, the free surface gives rise to higher stresses in the matrix and in the inclusion near the free surface for both interfacial conditions. Fig. 4 gives stress σ_{xx} and σ_{yy} along the x axis when the eigenstrain loading $\epsilon^*_{xx} = \epsilon^*_{zz} = 1$, $\epsilon^*_{yy} = 2\,\epsilon^*_{xx}$ is applied, $\Gamma = 100$ and $a = 0.8$ for the perfect bonding case. The effect of free surface is illustrated by comparing the stress field of the inclusion located near the free surface (solid lines) and of the inclusion embedded in the infinite matrix (dashed lines). Note that the stresses are uniform when a perfectly bonded inclusion is embedded in the infinite medium as expected from Eshelby's solution (Eshelby, 1957), but they cease to be uniform when the inclusion is located near the free surface. Fig. 5 illustrates the jump in the tangential displacement $[u_\theta]$ along the interface of the sliding inclusion for different eigenstrain loadings $\epsilon^*_{yy} = \epsilon^*_{xx}$, $\epsilon^*_{yy} = 2\epsilon^*_{xx}$ and $\epsilon^*_{yy} = \epsilon^*_{xx}/2$, while $\epsilon^*_{zz} = \epsilon^*_{xx}$, and $\Gamma = 100$, when the inclusion is located a distance of one radius away from the free surface ($a = 0.5$). Note that the free surface influences the degree of sliding. It is interesting to observe that the sliding occurs for the dilatational eigenstrain loading for the half-space problem, while in the infinite space the sliding cylindrical inclusion would experience no sliding due to this symmetric eigenstrain

loading. Fig. 6 shows the shear stress along the interface of the perfectly bonded inclusion for the above eigenstrain loadings. Fig. 7 gives the displacement u_x along the free surface for $0 \leq y \leq 1$ for both perfect bonding (dashed lines) and sliding (solid lines) cases, when a remote uniaxial loading is applied. The inclusion is embedded a distance of one radius away from the free boundary, which implies a = 0.5. Note that the displacement is significantly affected by Γ. The influence of interface can also be observed. The determination of the displacements at the free surface can be of interest to experimentalists since the differential strains can be measured by the experimental techniques such as stereoscopy and interference microscopy (Cox et al., 1988). These experimental and theoretical results can be used as a nondestructive technique to predict the nature of the defects inside a material (Mura, 1985).

In this chapter, Papkovich-Neuber displacement potentials in an infinite integral form and infinite series in polar coordinates are used. One of the advantages of using displacement potentials for this problem is that the formulation is similar in both two and three dimensions (Ishiwata, 1986; Tsuchida and Mura, 1983). The other one is that we can get displacements directly, while Airy's stress function method demands integration of strain or stress to determine the displacements.

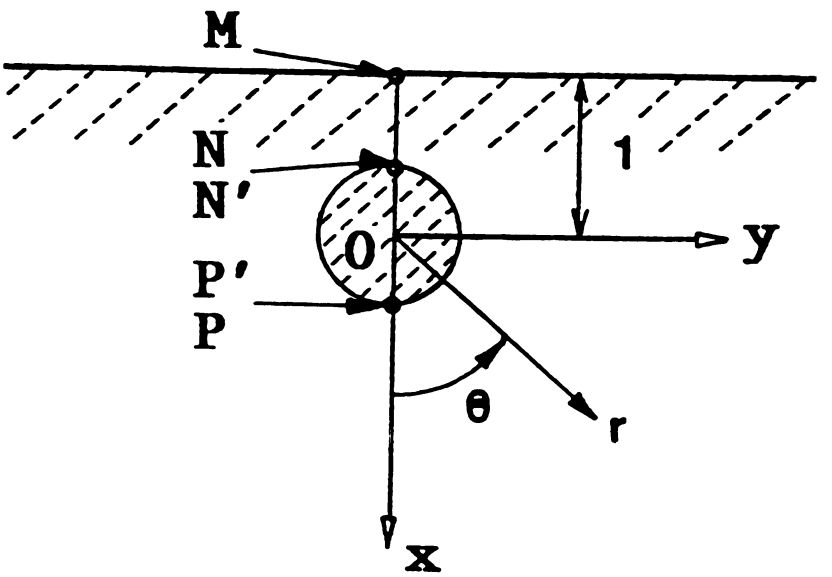

Fig. 1 Circular inclusion in a half-plane.

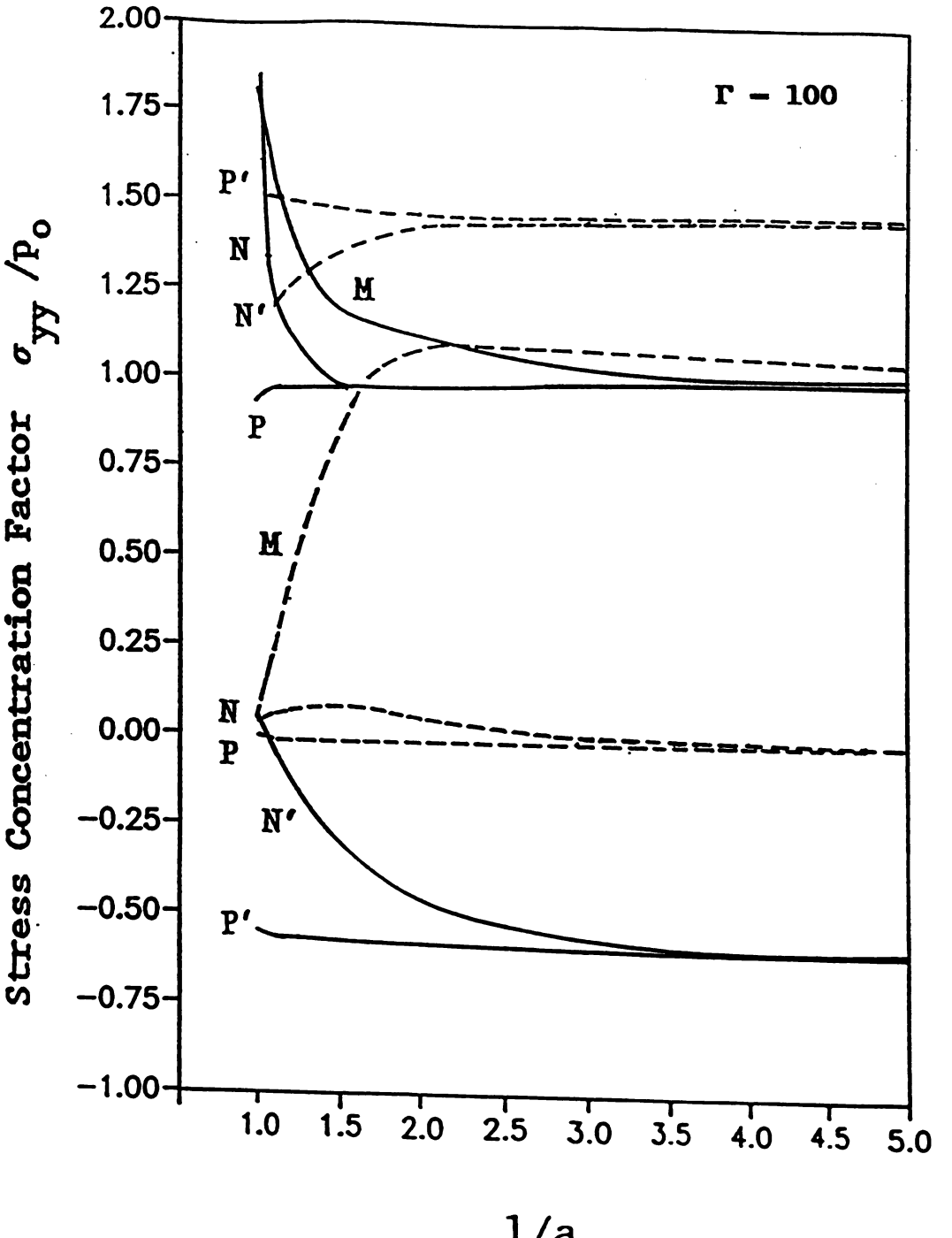

Fig. 2 σ_{yy} vs. 1/a for a uniaxial loading $\sigma_{yy} = p_o$ when $\Gamma = 100$ for perfect bonding case (dashed lines) and pure sliding (solid lines) for a half-plane case.

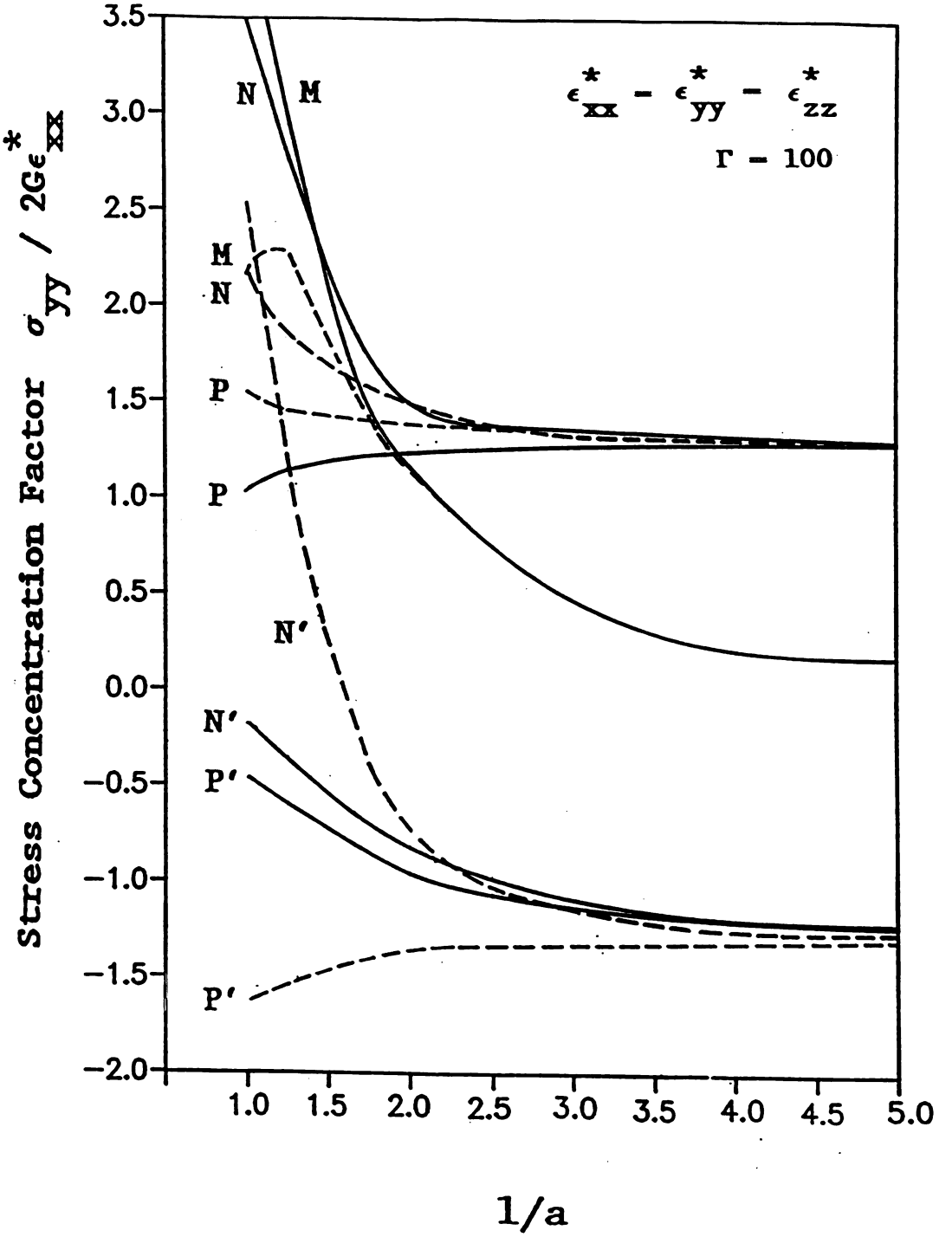

Fig. 3 σ_{yy} vs. 1/a for an eigenstrain loading $\epsilon^*_{xx} = \epsilon^*_{yy} = \epsilon^*_{zz}$ when Γ = 100 for perfect bonding (dashed lines) and pure sliding (solid lines) for a half-plane case.

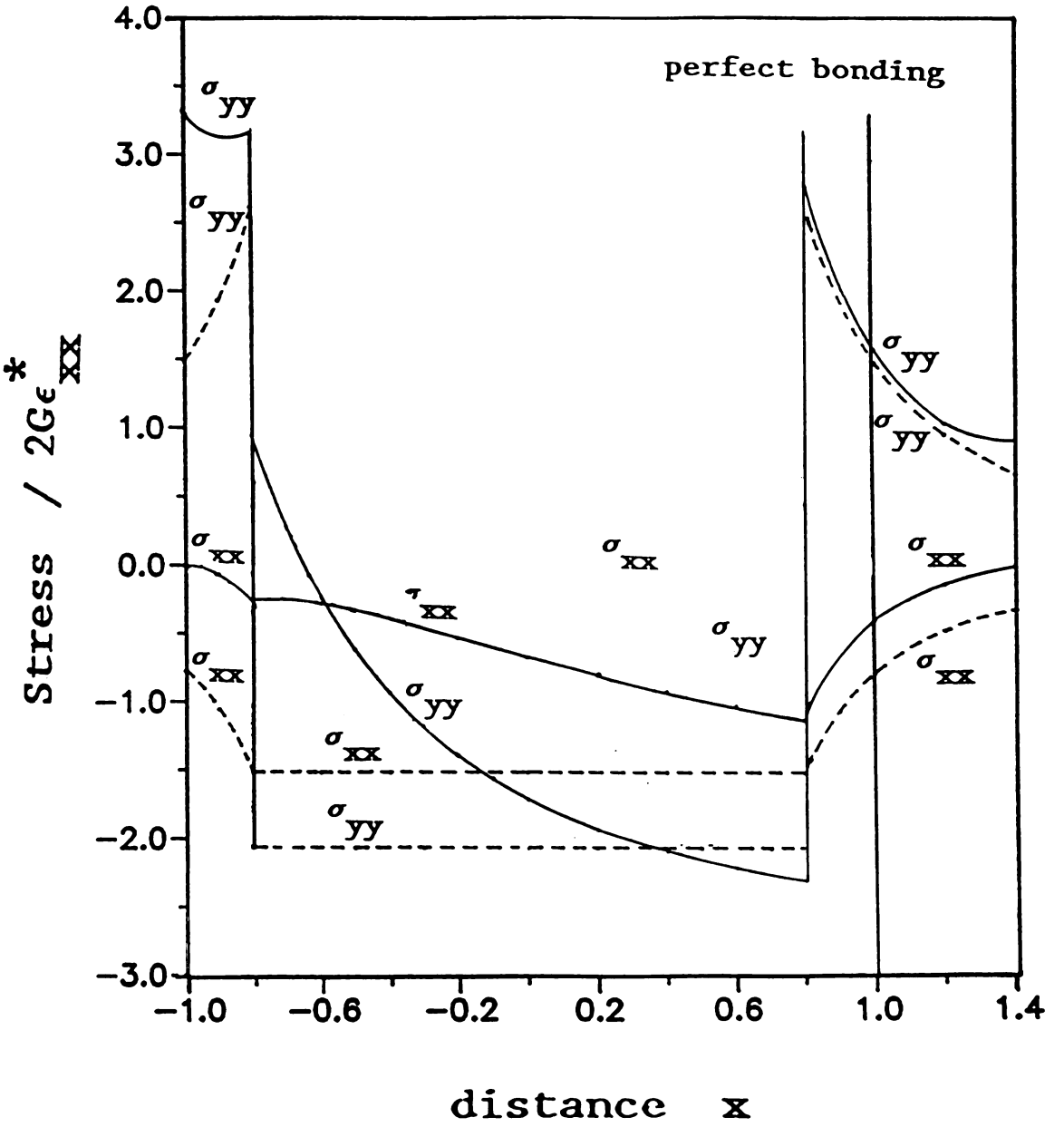

Fig. 4 σ_{xx} and σ_{yy} along x axis for eigenstain loading $\epsilon^*_{xx} = \epsilon^*_{zz}$, $\epsilon^*_{yy} = 2\,\epsilon^*_{xx}$ when $\Gamma = 100$ and $a = 0.8$. Solid lines represent the case when an inclusion is located near the free surface, while the dashed lines correspond to the case, when the inclusion is embedded in the infinite medium.

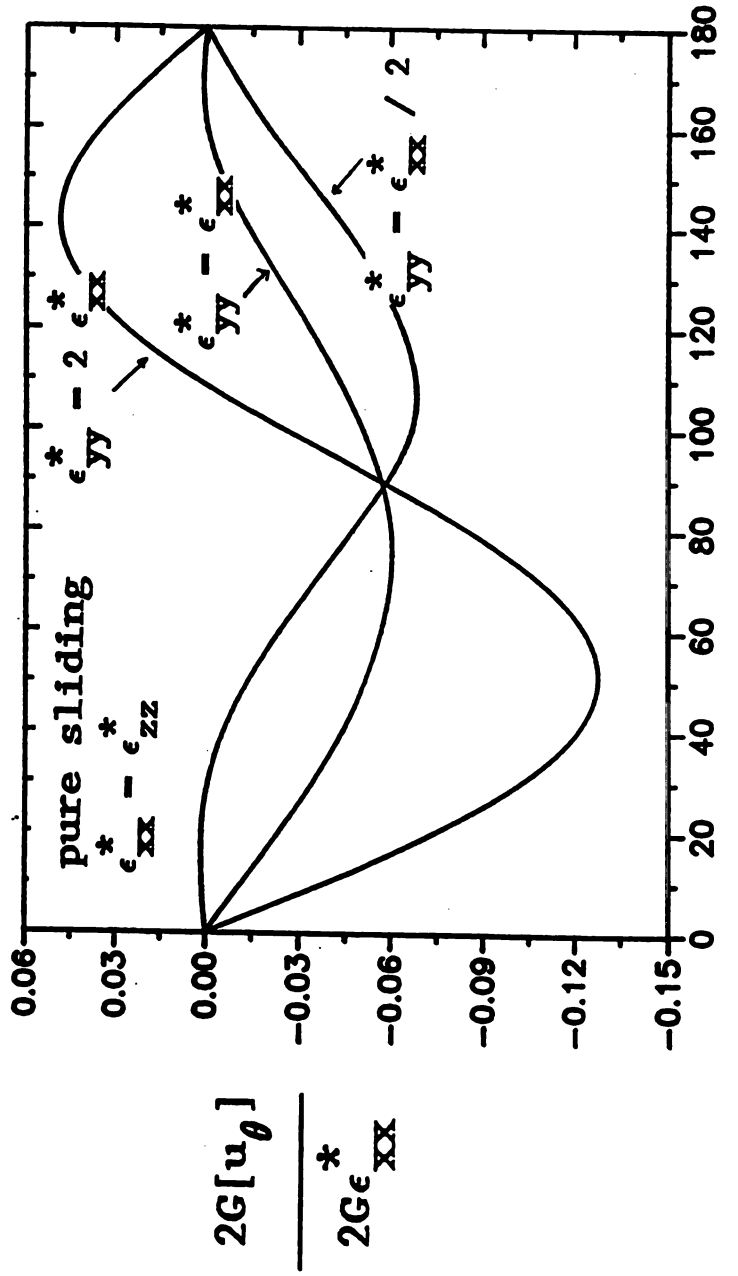

Fig. 5 Jump in the tangential displacement $[u_\theta]$ along the inclusion-matrix interface for eigenstain loading when $\Gamma = 100$ and $a = 0.5$ for half-plane.

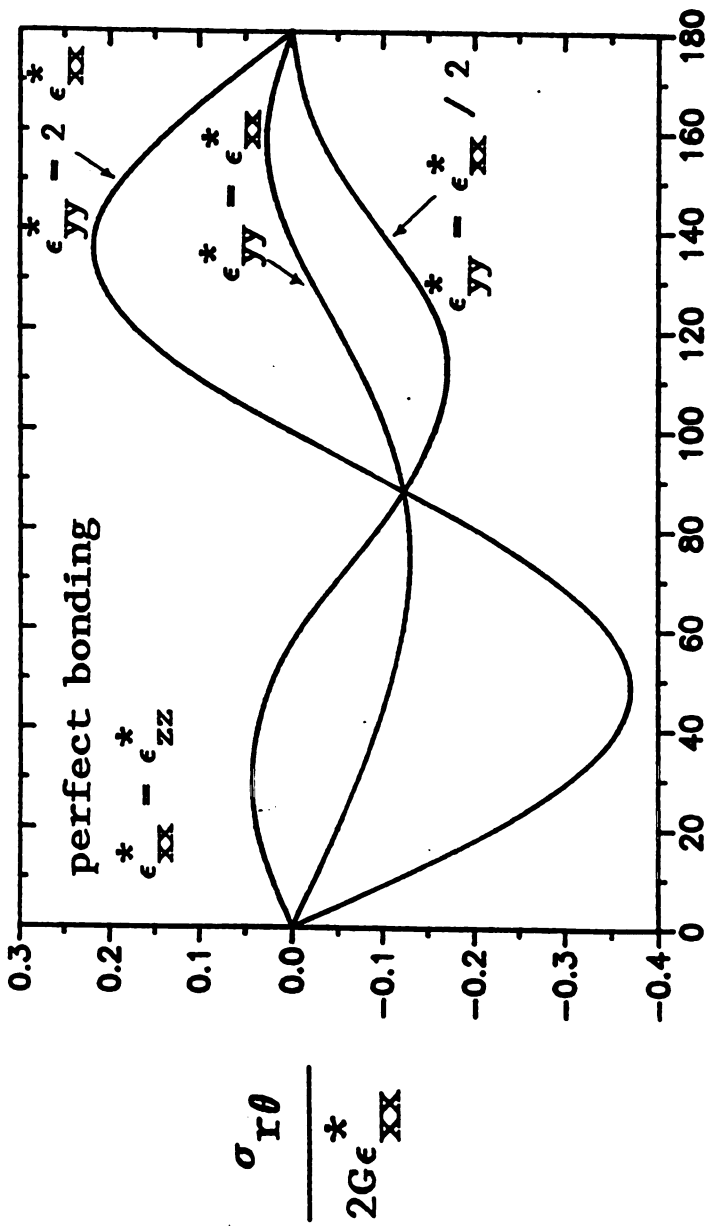

Fig. 6 Shear stress $\sigma_{r\theta}$ vs. θ for eigenstrain loading when $\Gamma = 100$ (perfect bonding case) for a half-plane case.

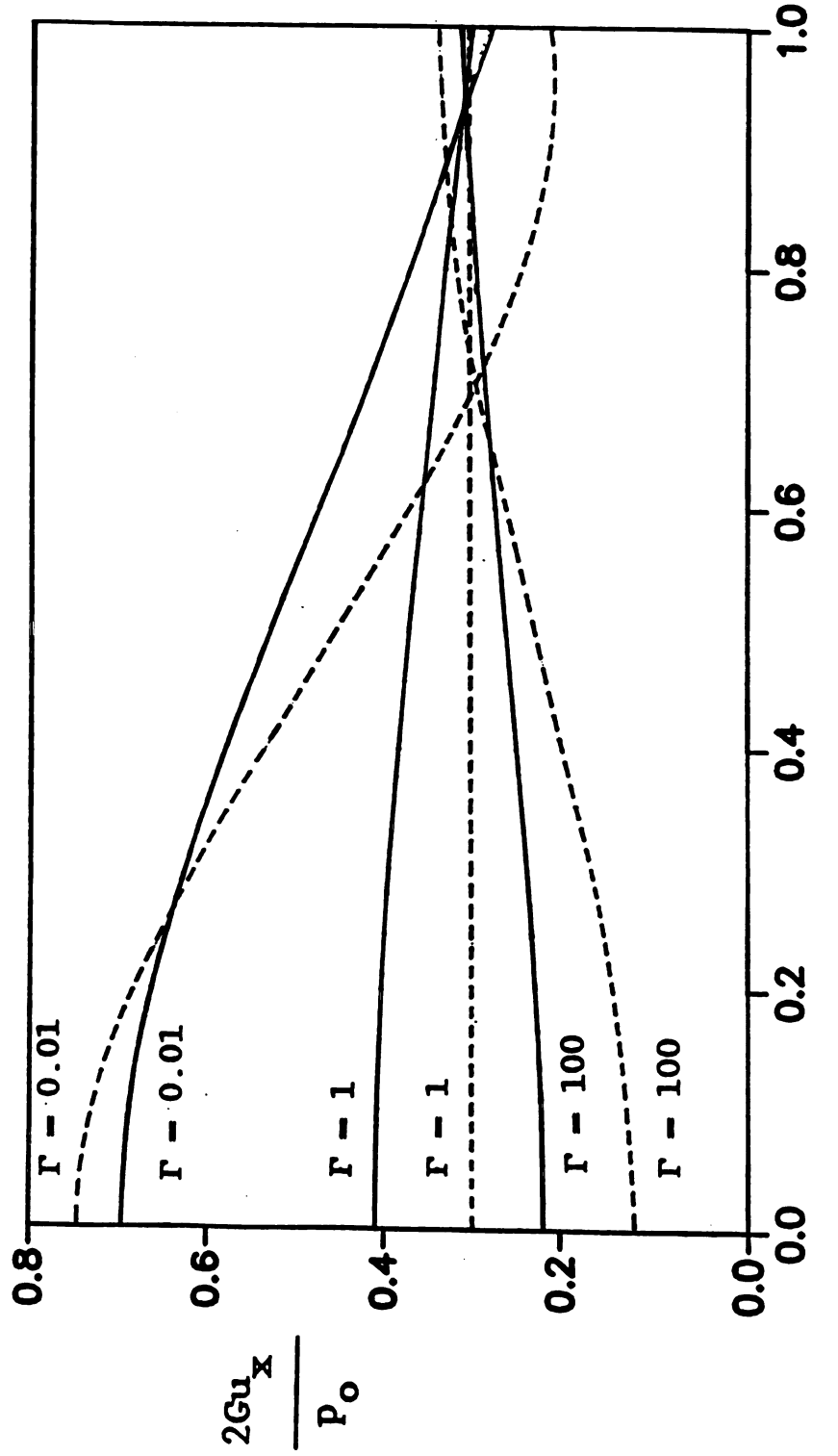

Fig. 7 Displacement u_x along the free surface for a uniaxial loading for a half-plane case. (x = -1)

CHAPTER 3 : A Circular Inclusion in an Infinite Strip

INTRODUCTION

In this part of dissertation, the plane elasticity problem of a circular inclusion embedded in an infinite strip is considered. The method of solution is similar to the previous problem (the case of inclusion in a half-plane discussed in Chapter 2). For completeness we include the details in this chapter. The solution will apply to two physical cases of a disk-like inclusion embedded in a thin strip (plane stress), or a cylindrical inclusion embedded in a very thick strip (plane strain).

METHOD OF SOLUTION

A circular inclusion in an infinite strip under either a uniaxial loading at infinity parallel to the edge boundaries, or a uniform non-shear type eigenstrain (transformation strain) is considered.

Let the origin of coordinates be at the center of the circular inclusion and the x-axis be directed down as shown in Fig. 8. The inclusion is assumed to be located an equal distance between two surfaces and the distance between the center of inclusion and the points on the free boundaries closest to the inclusion is taken as unity. Therefore, the free surfaces (the edges of the strip) are given by $x = \pm 1$. The radius of inclusion is taken as $r = a$.

The following boundary conditions are used:

i) the traction free condition on the surfaces $x = -1$ and $x = 1$:

$$(\sigma_{xx})_{x=\pm 1} = (\sigma_{xy})_{x=\pm 1} = 0 \tag{3.1}$$

ii) either the pure sliding conditions at the interface of the inclusion:

$$(\sigma_{rr})_{r=a} = (\bar{\sigma}_{rr})_{r=a} ,$$

$$(\sigma_{r\theta})_{r=a} = (\bar{\sigma}_{r\theta})_{r=a} = 0 \tag{3.2}$$

$$(u_r)_{r=a} = (\bar{u}_r)_{r=a}$$

or the perfect bonding conditions at the interface of the inclusion:

$$(\sigma_{rr})_{r=a} = (\bar{\sigma}_{rr})_{r=a}$$

$$(\sigma_{r\theta})_{r=a} = (\bar{\sigma}_{r\theta})_{r=a} \tag{3.3}$$

$$(u_r)_{r=a} = (\bar{u}_r)_{r=a}$$

$$(u_\theta)_{r=a} = (\bar{u}_\theta)_{r=a}$$

iii) either a uniaxial stress applied at infinity:

$$\sigma_{xx} = 0, \qquad \sigma_{xy} = 0, \qquad \sigma_{yy} = p_o \tag{3.4}$$

or the vanishing tractions for eigenstrain case:

$$\sigma_{ij} = 0, \qquad i,j = x,y. \tag{3.5}$$

In the preceding expressions the quantities defined in the inclusion are denoted by a superior bar.

The Papkovich-Neuber displacement potentials are given as follows:

i) for the matrix ($r > a$), ϕ_0 and ϕ_1 as

$$\text{(I)} \qquad \begin{cases} \phi_0 = C_0 \left(-A_0 \log r + \sum_{m=1}^{\infty} A_m \dfrac{\cos 2m\theta}{r^{2m}} \right) \\ \phi_1 = C_0 \sum_{m=0}^{\infty} B_m \dfrac{\cos (2m+1)\theta}{r^{2m+1}} \end{cases} \tag{3.6}$$

$$\text{(II)} \qquad \begin{cases} \phi_0 = C_0 \int_0^{\infty} \psi_1(\lambda) \cosh \lambda x \cos \lambda y \, d\lambda \\ \phi_1 = C_0 \int_0^{\infty} \lambda \, \psi_2(\lambda) \sinh \lambda x \cos \lambda y \, d\lambda \end{cases} \tag{3.7}$$

ii) and for the inclusion ($r < a$), ϕ_0 and ϕ_1 as

$$\text{(III)} \qquad \begin{cases} \phi_0 = C_0 \sum_{n=0}^{\infty} \bar{A}_n r^{2n} \cos 2n\theta \\ \phi_1 = C_0 \sum_{n=0}^{\infty} \bar{B}_n r^{2n+1} \cos (2n+1)\theta \end{cases} \tag{3.8}$$

where

$$C_0 = \begin{cases} p_o & \text{for a uniaxial loading} \\ 2G\epsilon^* & \text{for an eigenstrain loading} \quad (\epsilon^* = \epsilon^*_{xx}, \ \epsilon^*_{yy} \text{ or } \epsilon^*_{zz}) \end{cases}$$

where G is the shear modulus of the matrix and ϵ^*_{xx}, ϵ^*_{yy} and ϵ^*_{zz} are the eigenstrains. A_m, B_m, $\bar{A}_n$ and $\bar{B}_n$ are the unknown constants and $\psi_1(\lambda)$ and $\psi_2(\lambda)$ are the unknown functions of λ, which are determined from the

boundary conditions (3.1)-(3.5). Note that (I) is expressed by a suffix m and (III) by a suffix n.

When a uniaxial loading is applied, the displacement potentials are given as

$$\text{(IV)} \qquad \begin{cases} \phi_0 = \dfrac{p_o}{8}(\kappa+1)(y^2 - x^2) \\ \phi_1 = -\dfrac{p_o}{2} x \end{cases} \tag{3.9}$$

where

$$\kappa = \begin{cases} 3 - 4\nu & \text{for plane strain} \\ \dfrac{3-\nu}{1+\nu} & \text{for plane stress} \end{cases} \tag{3.10}$$

where ν is Poisson's ratio. The stresses and displacements obtained from (3.9) are expressed in polar coordinates as

$$\begin{aligned} \sigma_{rr} &= p_o \frac{1}{2}(1 - \cos 2\theta) \\ \sigma_{r\theta} &= p_o \frac{1}{2} \sin 2\theta \\ \sigma_{\theta\theta} &= p_o \frac{1}{2}(1 + \cos 2\theta) \\ 2G\, u_r &= p_o \frac{r}{4}\{(\kappa-1) - 2\cos 2\theta\} \\ 2G\, u_\theta &= p_o \frac{r}{2} \sin 2\theta \end{aligned} \tag{3.11}$$

When the inclusion is subjected to an eigenstrain loading, the displacements inside the inhomogeneity are the sum of displacements in the inclusion if there would be no constraint from the matrix

$$u_r^* = \frac{r}{2}\{\, 2\eta\, \epsilon_{zz}^* + (\epsilon_{xx}^* + \epsilon_{yy}^*) + (\epsilon_{xx}^* - \epsilon_{yy}^*)\cos 2\theta \,\}$$

$$u_\theta^* = \frac{r}{2}(\, \epsilon_{yy}^* - \epsilon_{xx}^*)\sin 2\theta. \tag{3.12}$$

where

$$\eta = \begin{cases} \nu & \text{for plane strain} \\ 0 & \text{for plane stress} \end{cases} \tag{3.13}$$

and the displacements obtained from III. The stresses in the inhomogeneity are obtained from III.

Note, that the stress components derived from (I) and (II) vanish at infinity. Therefore, for the eigenstrain loading the boundary condition (3.5) is automatically satisfied. For the case of uniaxial loading, ϕ_0 and ϕ_1, given by (IV), yield the uniaxial tension p_o. Therefore, the boundary condition (3.4) is also automatically satisfied. To satisfy the traction free boundary condition (3.1) at the free surfaces, (I) is considered as follows:

(I)-1 $\qquad \phi_0 = -\, C_0\, A_0 \log r$

(I)-2
$$\begin{cases} \phi_0 = C_0 \sum_{m=1}^{\infty} A_m \dfrac{\cos 2m\theta}{r^{2m}} \\ \phi_0 = C_0 \sum_{m=0}^{\infty} B_m \dfrac{\cos (2m+1)\theta}{r^{(2m+1)}} \end{cases} \tag{3.14}$$

Using two of the following mathematical relations

$$\frac{\cos m\theta}{r^m} = \frac{(-1)^m}{(m-1)!}\int_0^\infty \lambda^{m-1} e^{\lambda x}\cos \lambda y\, d\lambda$$

$$\frac{\sin m\theta}{r^m} = \frac{(-1)^{m-1}}{(m-1)!}\int_0^\infty \lambda^{m-1} e^{\lambda x}\sin \lambda y\, d\lambda, \qquad (x < 0) \quad (3.15)$$

$$\frac{\cos m\theta}{r^m} = \frac{1}{(m-1)!}\int_0^\infty \lambda^{m-1} e^{-\lambda x}\cos \lambda y\, d\lambda$$

$$\frac{\sin m\theta}{r^m} = \frac{1}{(m-1)!}\int_0^\infty \lambda^{m-1} e^{-\lambda x}\sin \lambda y\, d\lambda \qquad (x > 0)$$

(I)-2 is expressed in Cartesian coordinates as

$$(I)\text{-}2^* \quad \begin{cases} \phi_0 = C_1 \sum_{m=1}^{\infty} \frac{(-1)^{2m}}{(2m-1)!} A \int_0^\infty \lambda^{2m-1} e^{\lambda x}\cos \lambda y\, d\lambda \\ \phi_1 = C_0 \sum_{m=0}^{\infty} \frac{(-1)^{2m}}{(2m)!} B_m \int_0^\infty \lambda^{2m} e^{\lambda x}\cos \lambda y\, d\lambda. \end{cases} \qquad \begin{matrix} (x < 0) \\ (3.16) \end{matrix}$$

λ will be replaced by $-\lambda$ if $x > 0$.

As for (I)-1,

$$\phi_0 = -C_0 A_0 \log r = -C_0 A_0 \frac{1}{2}\log (x^2 + y^2) \qquad (3.17)$$

and the stresses are obtained directly from equation (3.17) as

$$\sigma_{xx} = C_0 A_0 \frac{\cos 2\theta}{r^2}$$

$$\sigma_{xy} = C_0 A_0 \frac{\sin 2\theta}{r^2} \tag{3.18}$$

and using (3.15) they are expressed as

$$\sigma_{xx} = C_0 A_0 \int_0^\infty \lambda e^{\lambda x} \cos \lambda y \, d\lambda \qquad (x < 0)$$

$$\sigma_{xy} = C_0 A_0 \int_0^\infty \lambda e^{\lambda x} \sin \lambda y \, d\lambda. \tag{3.19}$$

$$\sigma_{xx} = C_0 A_0 \int_0^\infty \lambda e^{-\lambda x} \cos \lambda y \, d\lambda \qquad (x > 0)$$

$$\sigma_{xy} = C_0 A_0 \int_0^\infty \lambda e^{-\lambda x} \sin \lambda y \, d\lambda.$$

Using equations (3.7), (3.16) and (3.19), the boundary conditions (3.1) are written as

$$\left(\frac{\sigma_{xx}}{C_0}\right)_{x=\pm 1} = \int_0^\infty \lambda^2 \Big[\psi_1(\lambda) \cosh \lambda - \psi_2(\lambda)\left(\frac{2}{1+\nu} \cosh\lambda - \lambda \sinh\lambda\right) + \sum_{m=1}^{\infty} A_m \frac{(-1)^{2m}}{(2m-1)!} \lambda^{2m-1} e^{-\lambda} - \sum_{m=0}^{\infty} B_m \frac{1}{(2m)!}\left(\frac{\kappa+1}{2} + \lambda\right) \lambda^{2m-1} e^{-\lambda} + A_0 \lambda^{-1} e^{-\lambda} \Big] \cos \lambda y \, d\lambda = 0 \tag{3.20}$$

$$\pm \left(\frac{\sigma_{xy}}{C_0}\right)_{x=-1} = \int_0^\infty \lambda^2 \Big[\psi_1(\lambda) \sinh\lambda - \frac{\kappa-1}{2} \psi_2(\lambda) \sinh\lambda + \psi_2(\lambda)\lambda \cosh \lambda - \sum_{m=1}^{\infty} A_m \frac{(-1)^{2m}}{(2m-1)!} \lambda^{2m-1} e^{-\lambda} + \sum_{m=0}^{\infty} B_m \frac{(-1)^{2m-1}}{(2m)!}\left(\frac{\kappa-1}{2} + \lambda\right) \lambda^{2m-1} e^{-\lambda}$$

$$- A_0 \lambda^{-1} e^{-\lambda}] \sin \lambda y \, d\lambda = 0 \qquad (3.21)$$

Setting the quantities in the brackets in equations (3.20)-(3.21) to zero, two equations for the two unknowns $\psi_1(\lambda)$ and $\psi_2(\lambda)$ are obtained. Solving these equations, $\psi_1(\lambda)$ and $\psi_2(\lambda)$ are found as

$$\psi_1(\lambda) = A_0 \frac{(\kappa + e^{-2\lambda} - 2\lambda)}{\sinh 2\lambda + 2\lambda} \lambda^{-1} + \sum_{m=1}^{\infty} \frac{A_m}{(2m-1)!} \frac{\lambda^{2m-1} (\kappa + e^{-2\lambda} - 2\lambda)}{\sinh 2\lambda + 2\lambda}$$

$$+ \sum_{m=0}^{\infty} \frac{B_m}{(2m)!} \frac{(\kappa^2 - 1 - 4\lambda^2)\lambda^{2m-1}}{(\sinh 2\lambda + 2\lambda)\, 2} \qquad (3.22)$$

$$\psi_2(\lambda) = A_0 \frac{2\lambda^{-1}}{\sinh 2\lambda + 2\lambda} + \sum_{m=1}^{\infty} \frac{A_m}{(2m-1)!} \frac{2\lambda^{2m-1}}{\sinh 2\lambda + 2\lambda}$$

$$+ \sum_{m=0}^{\infty} \frac{B_m}{(2m)!} \frac{(\kappa - e^{-2\lambda} + 2\lambda)\lambda^{2m-1}}{\sinh 2\lambda + 2\lambda} \qquad (3.23)$$

In order to satisfy the boundary conditions (3.2) or (3.3) at the inclusion's interface, the following relations are used

$$\cosh \lambda x \cos \lambda y = \sum_{n=0}^{\infty} \frac{(\lambda r)^{2n}}{2n!} \cos 2n\theta \qquad (3.24)$$

$$\sinh \lambda x \cos \lambda y = \sum_{n=0}^{\infty} \frac{(\lambda r)^{2n+1}}{(2n+1)!} \cos(2n+1)\theta$$

(II) is rewritten by using equations (3.24) as follows

$$(II)^* \quad \begin{cases} \phi_0 = C_0 \sum_{n=0}^{\infty} \alpha_n r^{2n} \cos 2n\theta \\ \phi_1 = C_0 \sum_{n=0}^{\infty} \beta_n r^{2n+1} \cos(2n+1)\theta \end{cases} \tag{3.25}$$

where

$$\alpha_n = \int_0^{\infty} \psi_1(\lambda) \frac{\lambda^{2n}}{2n!} d\lambda \tag{3.26}$$

$$\beta_n = \int_0^{\infty} \lambda \psi_2(\lambda) \frac{\lambda^{2n+1}}{(2n+1)!} d\lambda$$

and

$$\alpha_n = A_0 \alpha_{n1} + \sum_{m=1}^{\infty} \alpha_{n2}^m A_m + \sum_{m=0}^{\infty} \alpha_{n3}^m B_m$$

$$\beta_n = A_0 \beta_{n1} + \sum_{m=1}^{\infty} \beta_{n2}^m A_m + \sum_{m=0}^{\infty} \beta_{n3}^m B_m \tag{3.27}$$

where

$$\alpha_{n1} = \int_0^{\infty} (\kappa + e^{-2\lambda} - 2\lambda) \frac{\lambda^{2n-1}}{(2n)!} \frac{1}{\sinh 2\lambda + 2\lambda} d\lambda$$

$$\alpha_{n2}^m = \int_0^{\infty} \frac{(\kappa + e^{-2\lambda} - 2\lambda)}{(2n)!\ (2m-1)!} \lambda^{2n+2m-1} \frac{1}{\sinh 2\lambda + 2\lambda} d\lambda$$

$$\alpha_{n3}^m = \int_0^{\infty} \frac{(\kappa^2 - 1 - 4\lambda^2)}{2} \frac{\lambda^{2n+2m-1}}{(2n)!(2m)!} \frac{1}{\sinh 2\lambda + 2\lambda} d\lambda$$

$$\beta_{n1} = \int_0^\infty \frac{\lambda^{2n+1}}{(2n+1)!} \frac{2}{\sinh 2\lambda + 2\lambda} d\lambda \tag{3.28}$$

$$\beta_{n2}^m = \int_0^\infty \frac{\lambda^{2n+2m+1}}{(2n+1)!(2m-1)!} \frac{2}{\sinh 2\lambda + 2\lambda} d\lambda$$

$$\beta_{n3}^m = \int_0^\infty (\kappa - e^{-2\lambda} + 2\lambda) \frac{\lambda^{2m+2n+1}}{(2m)!(2n+1)!} \frac{1}{\sinh 2\lambda + 2\lambda} d\lambda$$

Using these relations

$$I_k = \int_0^\infty \frac{\lambda^k}{\sinh 2\lambda + 2\lambda} d\lambda \tag{3.29}$$

and

$$M_k = \int_0^\infty \frac{\lambda^{k_e - 2\lambda}}{\sinh 2\lambda + 2\lambda} d\lambda \tag{3.30}$$

equations (3.28) can be simplified as

$$\alpha_{n1}^m = \frac{1}{(2n)!(2m-1)!} [\kappa I_{2m+2n-1} + M_{2m+2n-1} - 2 I_{2m+2n}]$$

$$\alpha_{n2}^m = \frac{1}{(2n)!(2m-1)!} [\frac{\kappa^2 - 1}{2} I_{2m+2n-1} - 2I_{2m+2n+1}]$$

$$\alpha_{n0} = \frac{1}{(2n)!} [\kappa I_{2n-1} + M_{2n-1} - 2 I_{2n}] \tag{3.31}$$

$$\beta_{n1}^{m} = \frac{1}{(2n+1)(2m-1)!}\,[2\ I_{2m+2n+1}]$$

$$\beta_{n2}^{m} = \frac{1}{(2m)!(2n+1)!}\,[\kappa\ I_{2m+2n+1} - M_{2m+2n+1} + 2\ I_{2m+2n+2}]$$

$$\beta_{n0} = \frac{1}{(2n+1)!}\,[2\ I_{2n+1}]$$

Next, the stresses and displacements are derived from the displacement potentials given by (I), (II)* and (III), and the equations (3.11) are used for uniaxial loading and equations (3.12) for eigenstrain loading cases. Substituting these results in the sliding boundary conditions (3.2), the following four equations are obtained:

i) the continuity of normal tractions $(\sigma_{rr})_{r=a} = (\bar{\sigma}_{rr})_{r=a}$:

$$\sum_{n=0}^{\infty} [s_{A1}\ A_n + s_{B1}\ B_{n-1} + s_{B2}\ B_n + s_{\alpha 1}\ \alpha_n + s_{\beta 1}\ \beta_{n-1} + s_{\beta 2}\ \beta_n$$

$$- \bar{s}_{A1}\ \bar{A}_n - \bar{s}_{B1}\ \bar{B}_{n-1} - \bar{s}_{B2}\ \bar{B}_n\ ]\ \cos n\theta = -\ \frac{A_0}{a^2} - \frac{P_o}{C_0}\ \frac{(1-\cos 2\theta)}{2} \tag{3.32}$$

ii) the condition of continuity of normal displacements

$(u_r)_{r=a} = (\bar{u}_r)_{r=a}$:

$$\sum_{n=0}^{\infty} [\{k_{A1}\ A_n + k_{B1}\ B_{n-1} + k_{B2}\ B_n + k_{\alpha 1}\ \alpha_n + k_{\beta 1}\ \beta_{n-1} + k_{\beta 2}\ \beta_n\}$$

$$- \frac{1}{\Gamma}\ \{\bar{k}_{A1}\ \bar{A}_n + \bar{k}_{B1}\ \bar{B}_{n-1} + \bar{k}_{B2}\ \bar{B}_n\}\ ]\ \cos n\theta =$$

$$\frac{A_0}{a} - \frac{p_o}{C_0}\frac{a}{4}\{(1-\kappa) - 2\cos 2\theta\} +$$

$$\frac{2G}{C_0}\frac{a}{2}\{2\eta\,\epsilon^*_{zz} + (\epsilon^*_{xx} + \epsilon^*_{yy}) + (\epsilon^*_{xx} - \epsilon^*_{yy})\cos 2\theta\} \qquad (3.33)$$

iii) the continuity of tangential tractions $(\sigma_{r\theta})_{r=a} = (\bar{\sigma}_{r\theta})_{r=a}$:

$$\sum_{n=1}^{\infty}[t_{A1}A_n + t_{B1}B_{n-1} + t_{B2}B_n + t_{\alpha 1}\alpha_n + t_{\beta 1}\beta_{n-1} + t_{\beta 2}\beta_n$$

$$- \bar{t}_{A1}\bar{A}_n - \bar{t}_{B1}\bar{B}_{n-1} - \bar{t}_{B2}\bar{B}_n]\sin n\theta = -\frac{p_o}{C_0}\frac{1}{2}\sin 2\theta \qquad (3.34)$$

iv) and the condition of vanishing shear tractions given by either

$(\bar{\sigma}_{r\theta})_{r=a} = 0$:

$$\sum_{n=1}^{\infty}[\bar{t}_{A1}\bar{A}_n + \bar{t}_{B1}\bar{B}_{n-1} + \bar{t}_{B2}\bar{B}_n]\sin n\theta = 0 \qquad (3.35)$$

or $(\sigma_{r\theta})_{r=a} = 0$.

The problem of perfectly bonded inclusion can be solved by using the first three equations, (3.34)-(3.36), and the last one, (3.37), is replaced by the condition of continuity of tangential displacements

$(u_\theta)_{r=a} = (\bar{u}_\theta)_{r=a}$:

$$\sum_{n=1}^{\infty}[\{l_{A1}A_n + l_{B1}B_{n-1} + l_{B2}B_n + l_{\alpha 1}\alpha_n + l_{\beta 1}\beta_{n-1} + l_{\beta 2}\beta_n\}$$

$$- \frac{1}{\Gamma} \{ \bar{I}_{A1} \bar{A}_n + \bar{I}_{B1} \bar{B}_{n-1} + \bar{I}_{B2} \bar{B}_n \}] \sin n\theta = - \frac{p_o}{C_0} \frac{a}{2} \sin 2\theta$$

$$+ \frac{2G}{C_0} \frac{a}{2} (\epsilon^*_{yy} - \epsilon^*_{xx}) \sin 2\theta \qquad (3.36)$$

where $\Gamma = \bar{G} / G$, and G and $\bar{G}$ are the shear moduli of the matrix and inclusion, respectively, and

$$k_{A1} = \frac{-2n}{a^{2n+1}}, \qquad k_{B1} = \frac{-(2n-1+\kappa)}{2a^{2n-1}}, \qquad k_{B2} = \frac{-(2n+1+\kappa)}{2a^{2n+1}},$$

$$k_{\alpha 1} = 2na^{2n-1}, \qquad k_{\beta 1} = \frac{(2n-1-\kappa)a^{2n-1}}{2}, \qquad k_{\beta 2} = \frac{(2n+1-\kappa)a^{2n+1}}{2} \qquad (3.37)$$

$$l_{A1} = \frac{-2n}{a^{2n+1}}, \qquad l_{B1} = \frac{-(2n-1-\kappa)}{2a^{2n-1}}, \qquad l_{B2} = \frac{-(2n+1+\kappa)}{2a^{n+1}},$$

$$l_{\alpha 1} = (-2n)\, a^{2n-1}, \qquad l_{\beta 1} = \frac{(\kappa-2n+1)a^{2n-1}}{2}, \qquad l_{\beta 2} = \frac{-(\kappa+2n+1)a^{2n+1}}{2} \qquad (3.38)$$

$$s_{A1} = \frac{2n(2n+1)}{a^{2n+2}}, \qquad s_{B1} = \frac{(2n-1)(2n+2)}{2a^{2n}}, \qquad s_{B2} = \frac{(2n+1)(2n+1+\kappa)}{2a^{n+2}},$$

$$s_{\alpha 1} = 2n(2n-1)a^{2n-2}, \quad s_{\beta 1} = \frac{(2n-1)(2n-1-\kappa)\, a^{2n-2}}{2}, \quad s_{\beta 2} = \frac{(2n+1)(2n-2)a^{2n}}{2} \qquad (3.39)$$

$$t_{A1} = \frac{2n(2n+1)}{a^{2n+2}}, \qquad t_{B1} = \frac{2n(2n-1)}{2a^{2n}}, \qquad t_{B2} = \frac{(2n+1)(2n+1+\kappa)}{2a^{2n+2}}$$

$$t_{\alpha 1} = (-2n)(2n-1)a^{2n-2},\quad t_{\beta 1} = \frac{(1-2n)(2n-1-\kappa)\,a^{2n-2}}{2},\quad t_{\beta 2} = \frac{-(1+2n)2n\,a^{2n}}{2} \tag{3.40}$$

Note that the terms involving barred quantities $\bar{k}_{A1}$, $\bar{k}_{B1}$, $\bar{l}_{A1}$,... can be obtained directly from $k_{\alpha 1}$, $k_{\beta 1}$, $l_{\alpha 1}$,... by replacing κ with $\bar{\kappa}$.

Note that the equations (3.32)-(3.36) are same as the corresponding equations in Chapter 2 but equations (3.37)-(3.40) differ from the ones in Chapter 2. Equating the coefficients of sin $n\theta$ and cos $n\theta$ in the left and right sides of either equations (3.34)-(3.37) for the sliding case, or (3.34)-(3.36) and (3.38) for the perfect bonding case, an infinite set of algebraic equations for the unknown constants A_n, B_n, $\bar{A}_n$ and $\bar{B}_n$ is obtained.

RESULTS AND DISCUSSION

In this chapter the plane strain case is considered for numerical examples. ν and $\bar{\nu}$ are chosen to be 0.3. Figs. 9-10 show the stresses σ_{yy} at points M, N and N′ (or P and P′) for both perfectly bonded case (dashed line) and pure sliding (solid line) case as the radius "a" of the inclusion is varied from 0.2 to 0.9. Comparison with the half-plane case given in Chapter 2 is included. As expected, the tendency of stress distribution is quite similar for both cases. For details, compare Figs. 2-3 with Figs. 9-10.

Fig. 11 shows that the stresses σ_{xx}, σ_{yy} along the x axis for eigenstrain loading $\epsilon^*_{xx} = \epsilon^*_{zz}$, $\epsilon^*_{yy} = 2\,\epsilon^*_{xx}$ when $\Gamma = 100$ and $a = 0.8$. Solid lines represent the case when an inclusion is located near the free surface, the point lines are for the case when the inclusion is in

the infinite strip, while the dashed lines correspond to the case, when the inclusion is embedded in the infinite medium. Note that the stresses in the half plane fall between the solutions for the infinite plane case and strip case as expected.

Next, the behavior of displacements on the free surfaces is investigated in Figs. 14-21. Figs. 14-15 illustrate the displacements on the free surfaces for perfect bonding and pure sliding cases for different positions of the inclusion relative to the free surface. The radius "a" is varied as 0.1, 0.5, and 0.9, while the center of the inclusion remains at the center of the strip. The loading condition is the remote uniaxial loading $\sigma_{yy} = p_o$. The soft inclusion ($\Gamma = 0.01$) has a more pronounced effect on the displacements of the free surfaces. That is simply because the softer inclusion can not sustain a uniaxial loading and it deforms more than the stiffer inclusion. When the inclusion is stiff ($\Gamma = 100$), the displacements for perfectly bonded case are less pronounced than those for pure sliding case. It means that pure sliding boundary condition actually helps the matrix to deform more freely so that the displacements on the free surfaces are much larger, comparatively.

The case of the eigenstrain loading (Figs. 16-21) has different features. The stiffer inclusion has more effect on the displacements along the free surfaces. The boundary condition does not contribute much unless the size of inclusion is large enough such as $a = 0.9$. It is interesting to observe that both boundary conditions have a very similar influence on the deformation along the free surfaces under any type of eigenstrain loading.

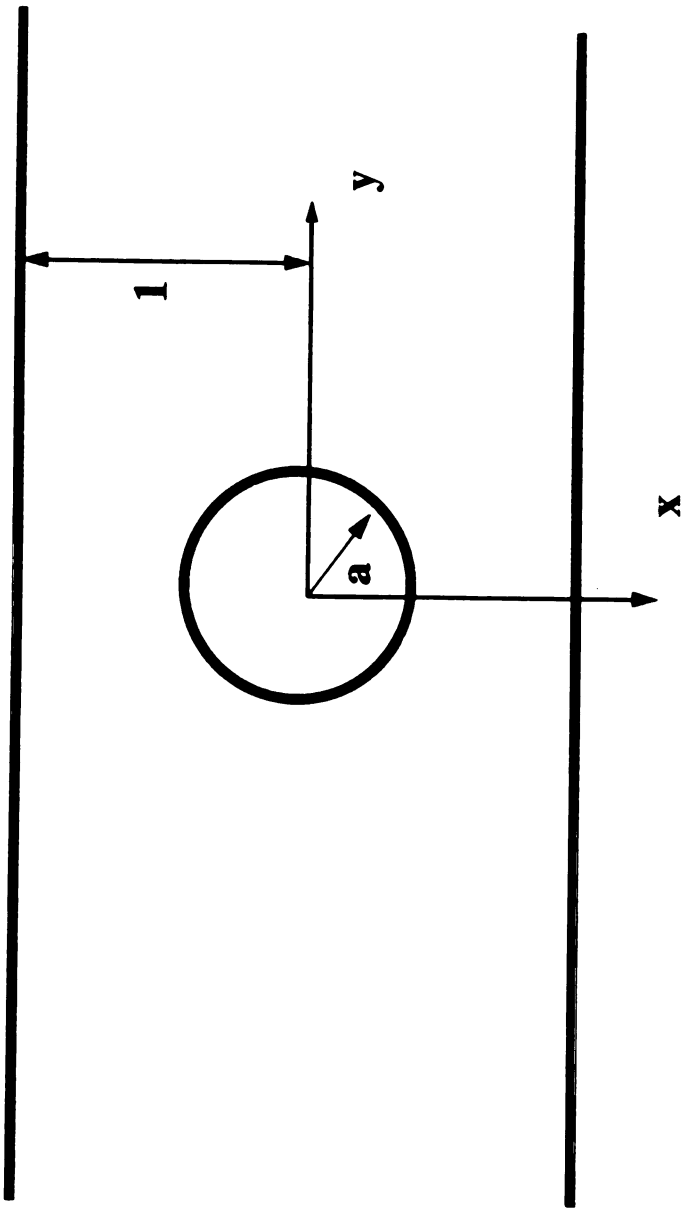

Fig. 8 Circular inclusion in an infinite strip

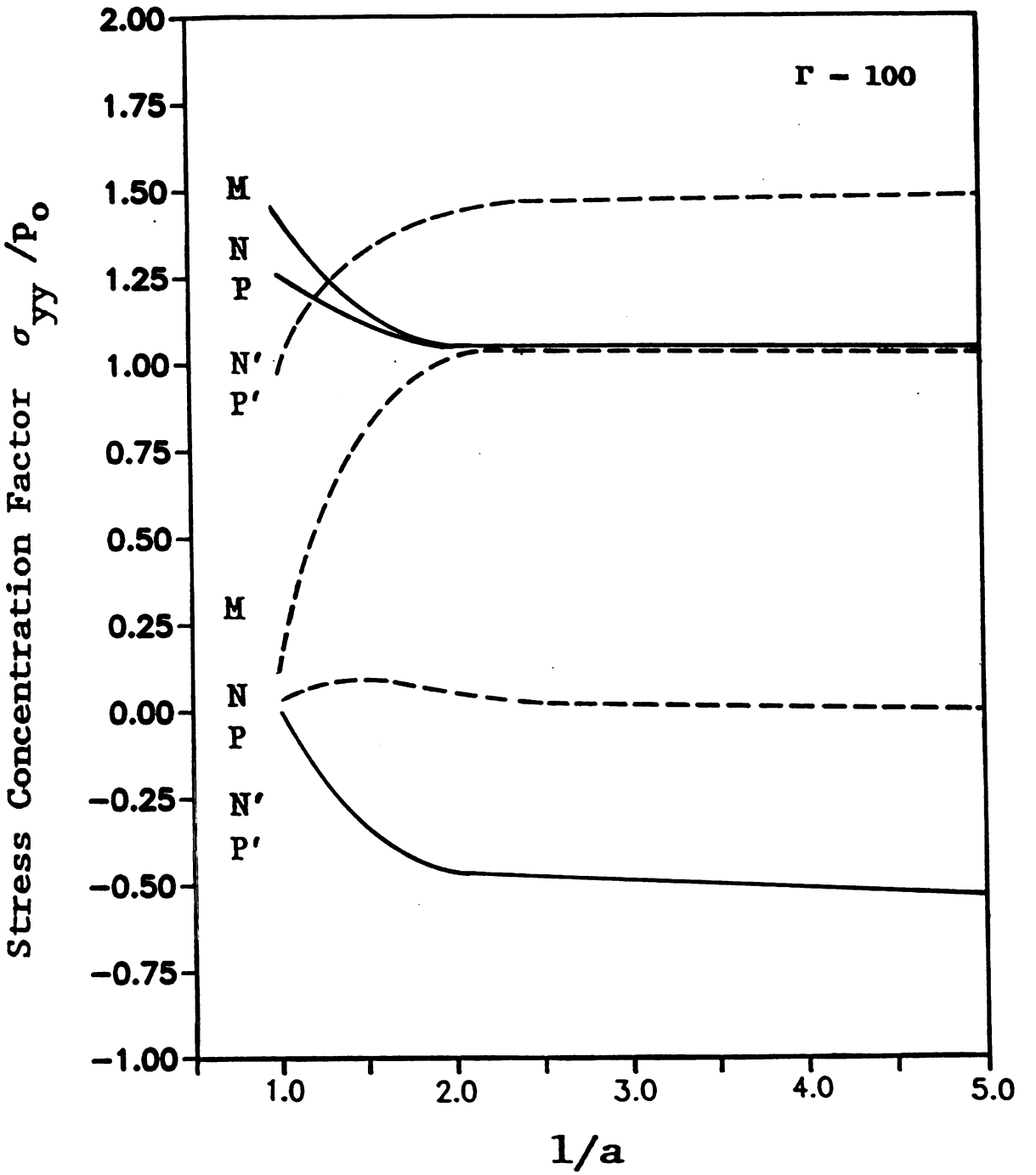

Fig. 9 σ_{yy} vs. 1/a for a uniaxial loading $\sigma_{yy} = p_o$ when $\Gamma = 100$ for for perfect bonding (dashed lines) and pure sliding (solid lines) for an infinite strip case.

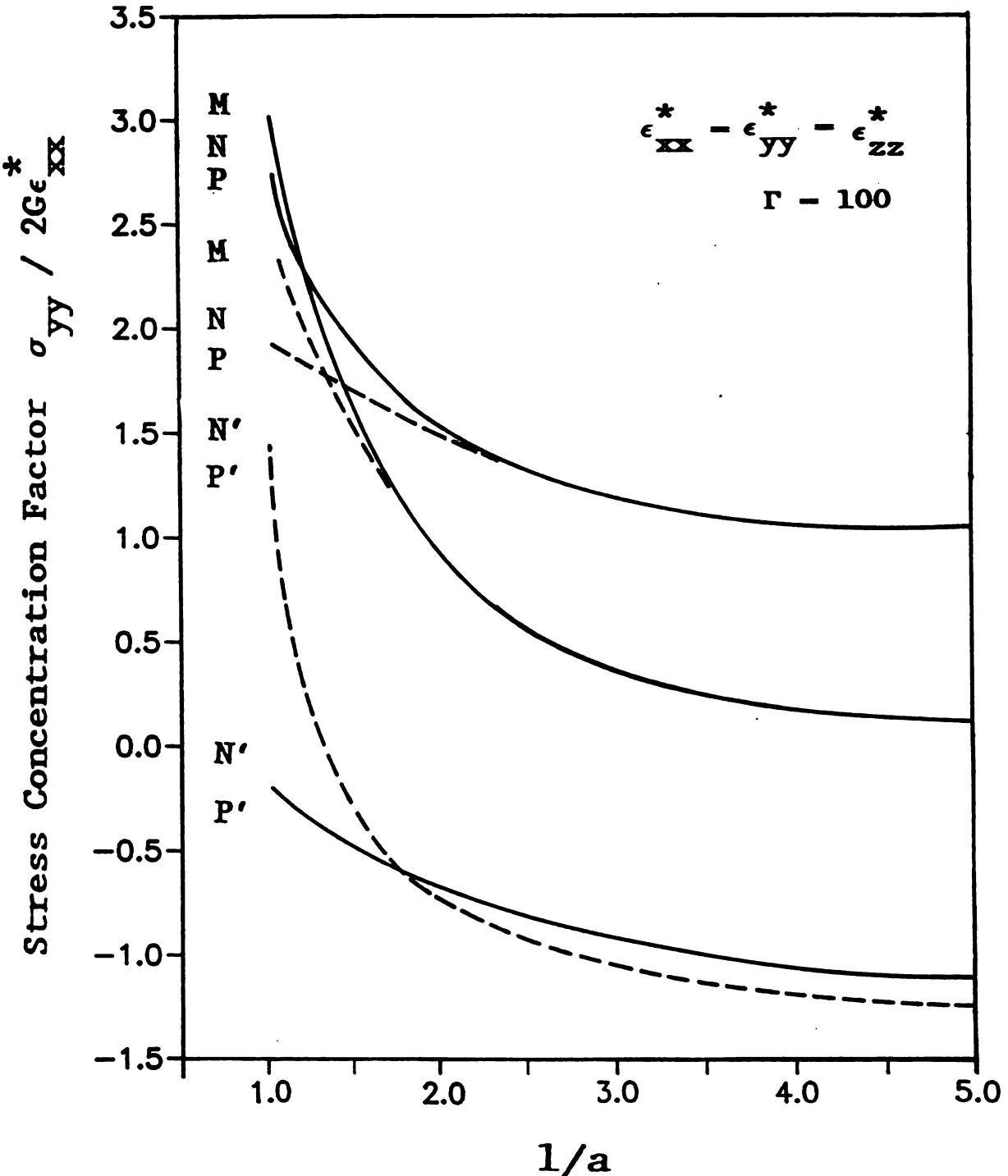

Fig. 10 σ_{yy} vs. 1/a for an eigenstrain loading $\epsilon^*_{xx} - \epsilon^*_{yy} - \epsilon^*_{zz}$ when Γ = 100 for perfect bonding (dashed lines) and pure sliding (solid lines) for an infinite strip case.

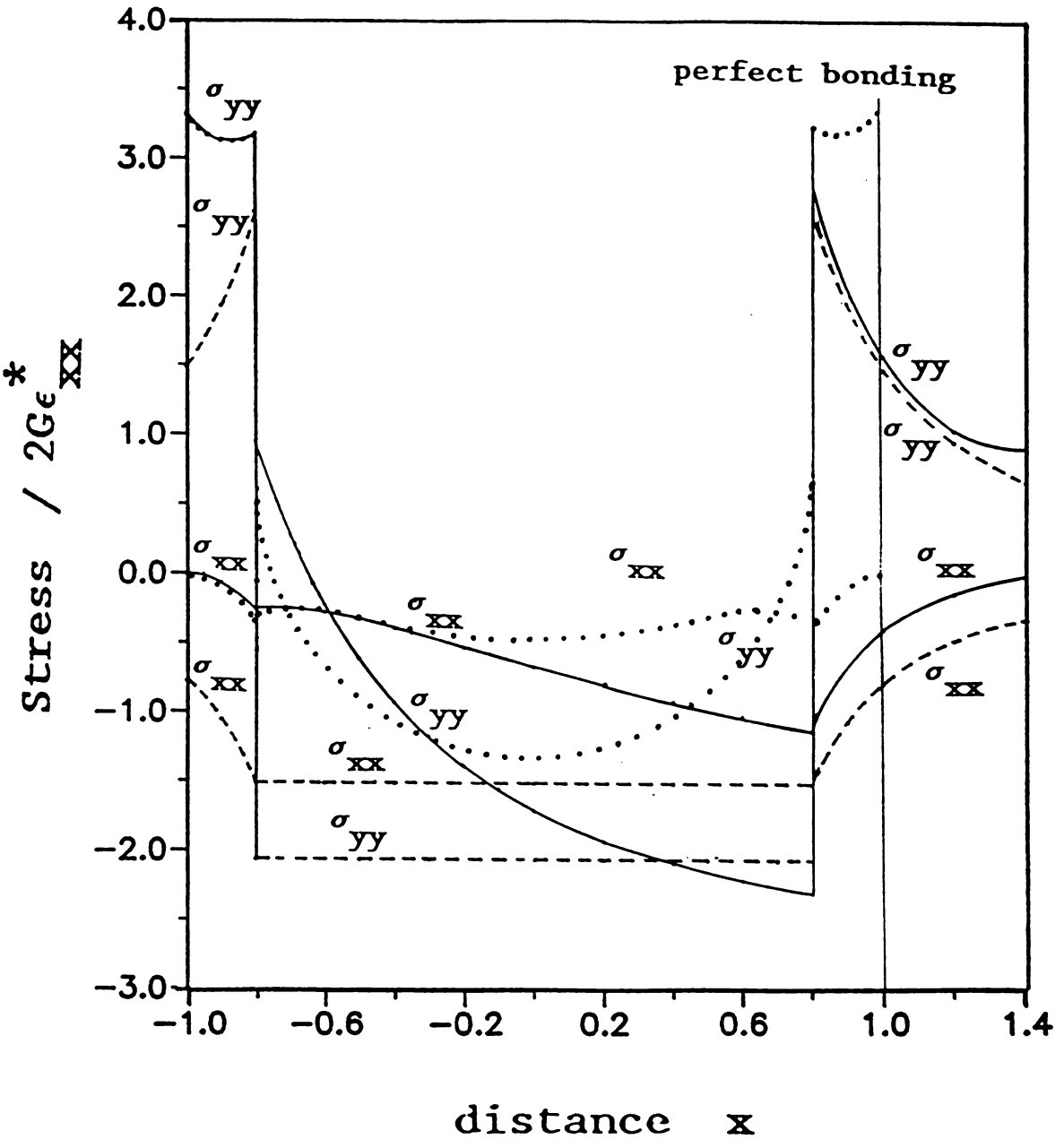

Fig. 11 σ_{xx} and σ_{yy} along x axis for eigenstain loading $\epsilon^*_{xx} = \epsilon^*_{zz}$, $\epsilon^*_{yy} = 2\,\epsilon^*_{xx}$. Solid lines represent the case when an inclusion is located near the free surface (a=0.8), point lines represent the case when an inclusion is embedded in the strip, while dashed lines correspond to the case, when the inclusion is embedded in the infinite medium.

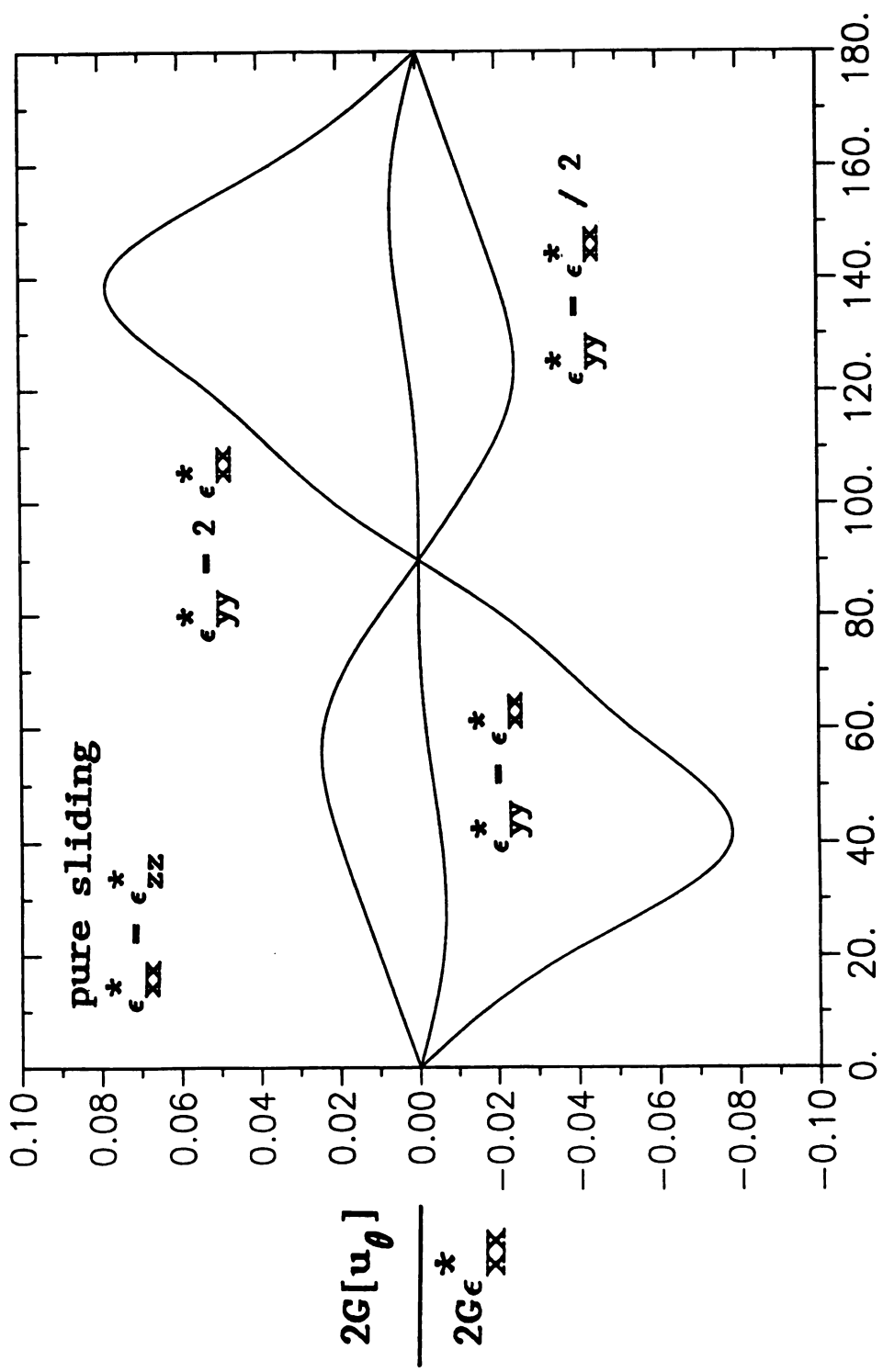

Fig. 12 Jump in the tangential displacement $[u_\theta]$ along the inclusion-matrix interface for eigenstrain loading when $\Gamma = 100$ and $a = 0.5$ (pure sliding case) for an infinite strip case.

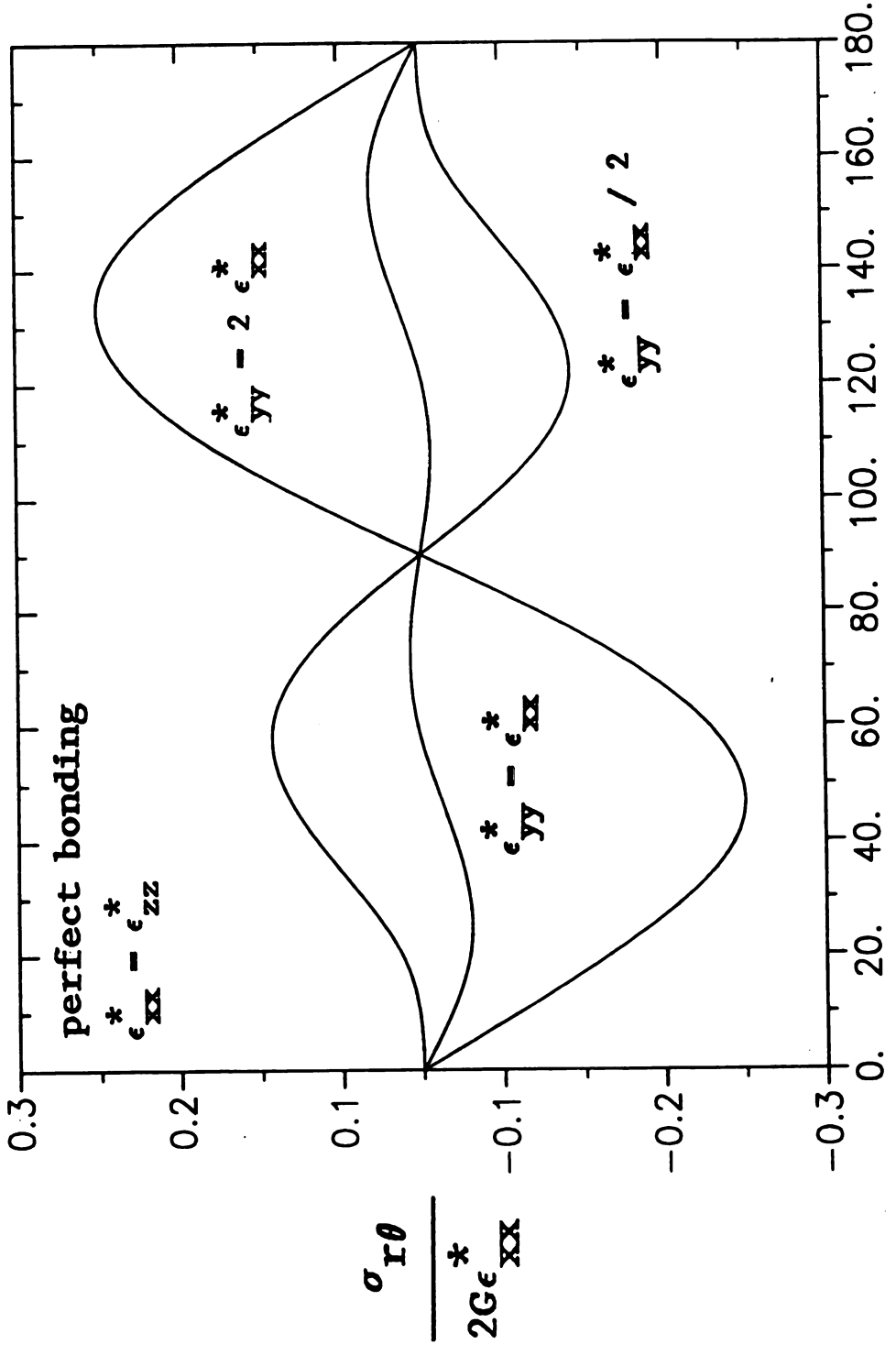

Fig. 13 Shear stress $\sigma_{r\theta}$ vs. θ for eigenstrain loading when $\Gamma = 100$ (perfect bonding case) for an infinite strip.

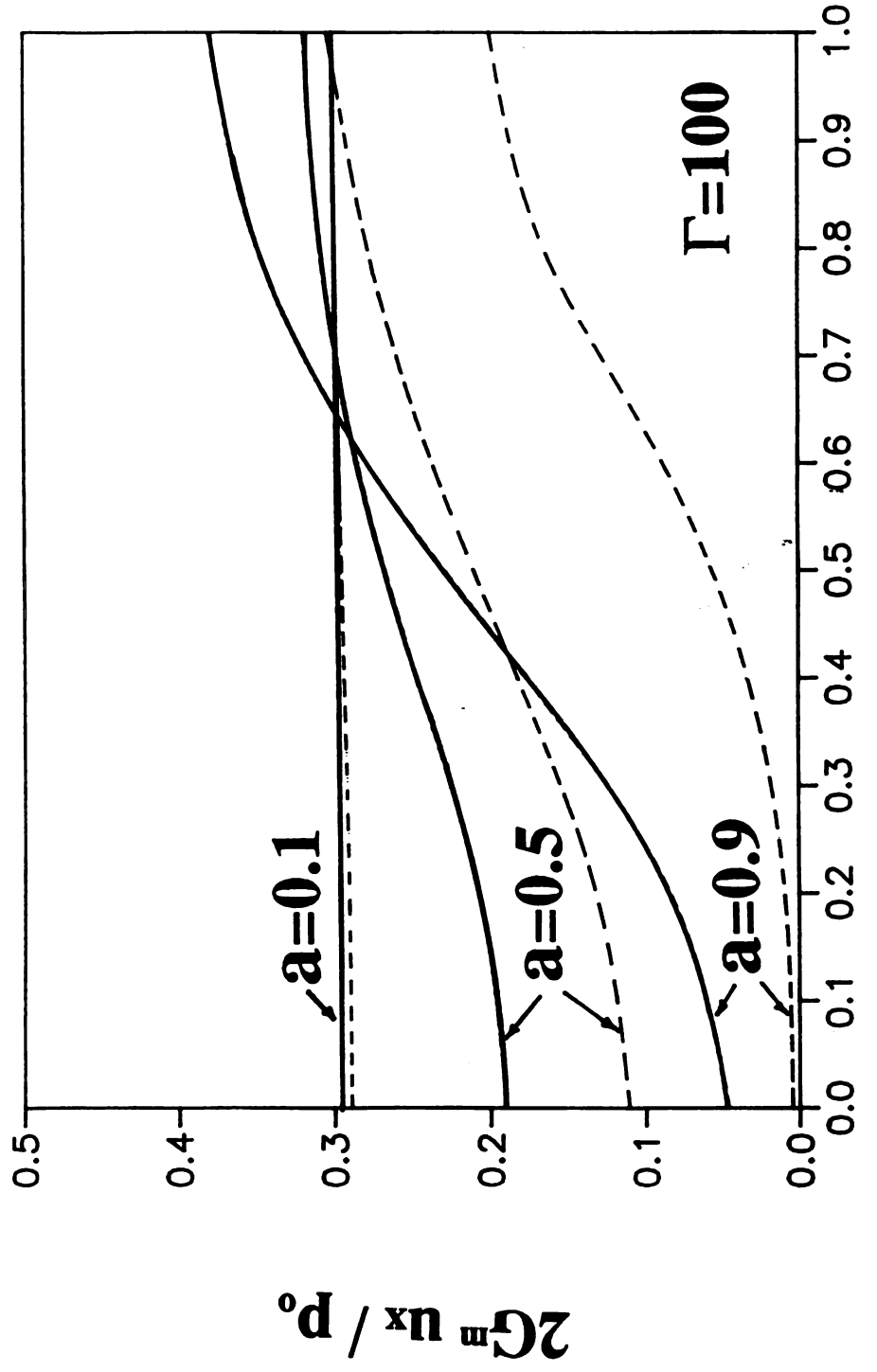

Fig. 14 Displacement u_x along the free surface for a uniaxial loading for an infinite strip case when $\Gamma = 100.(x = -1)$

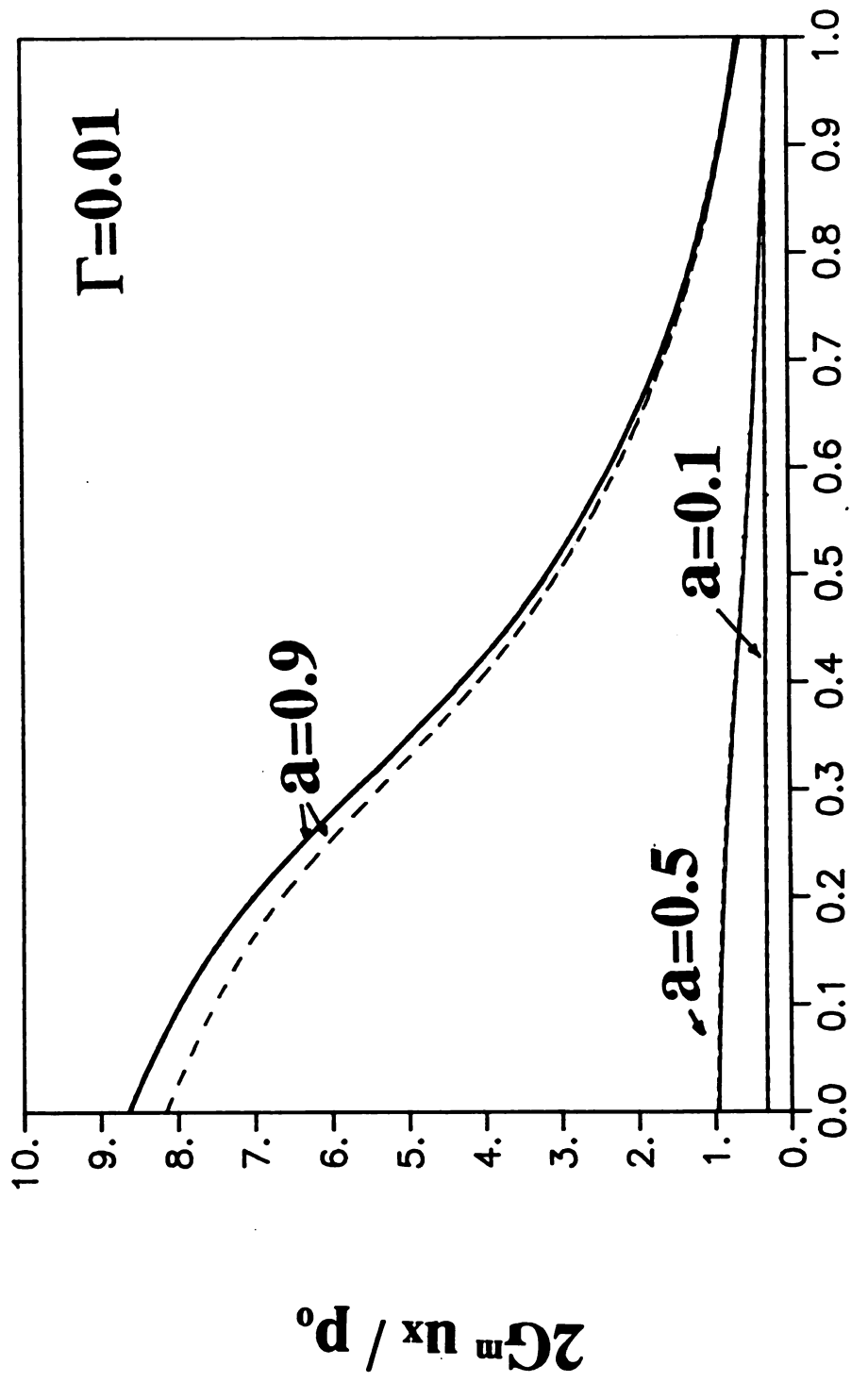

Fig. 15 Displacement u_x along the free surface for a uniaxial loading for an infinite strip case when $\Gamma = 0.01(x = -1)$

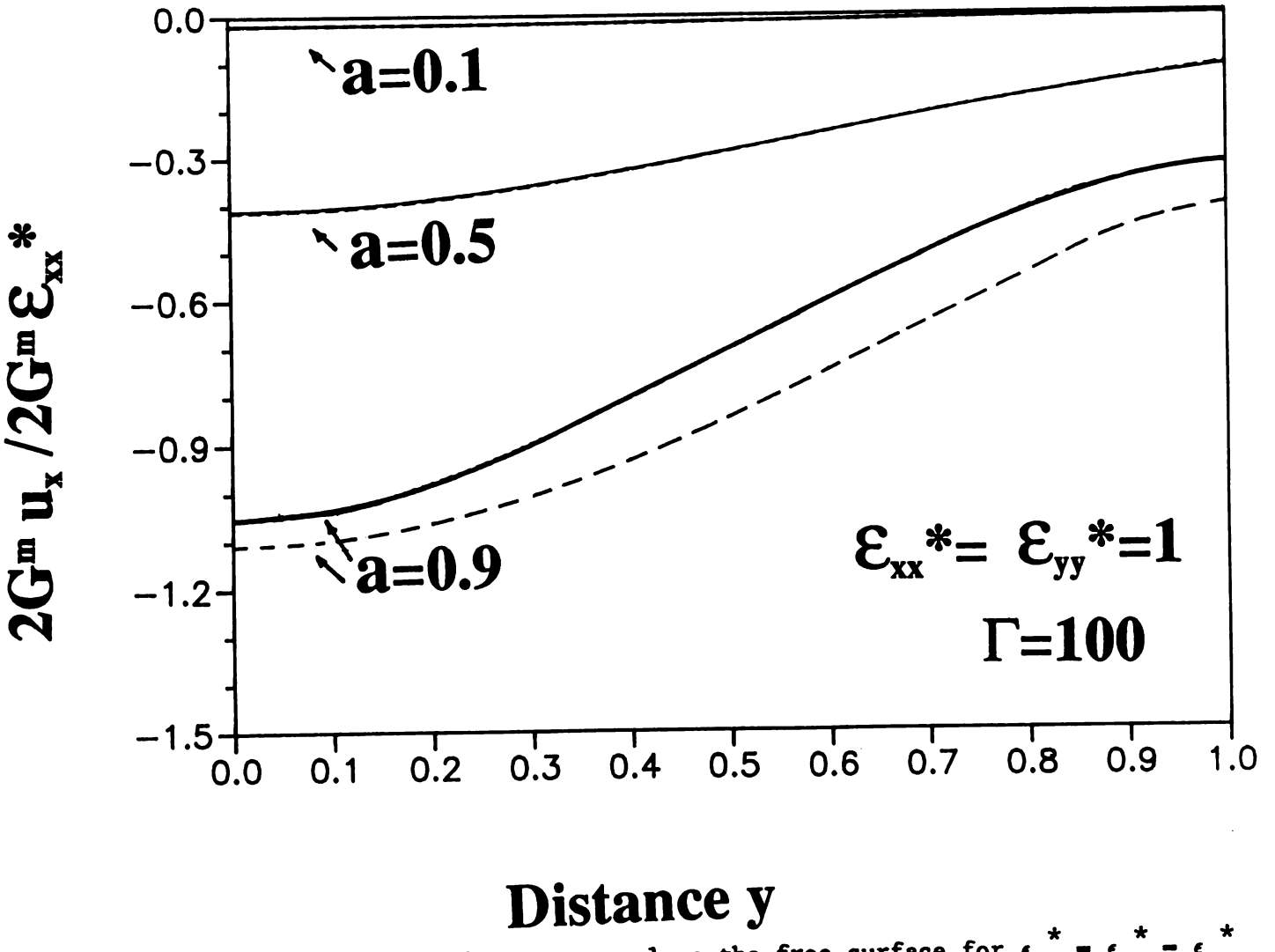

Fig. 16 Displacement u_x along the free surface for $\epsilon_{xx}^* = \epsilon_{yy}^* = \epsilon_{zz}^*$ for an infinite strip when $\Gamma = 100$. ($x = -1$)

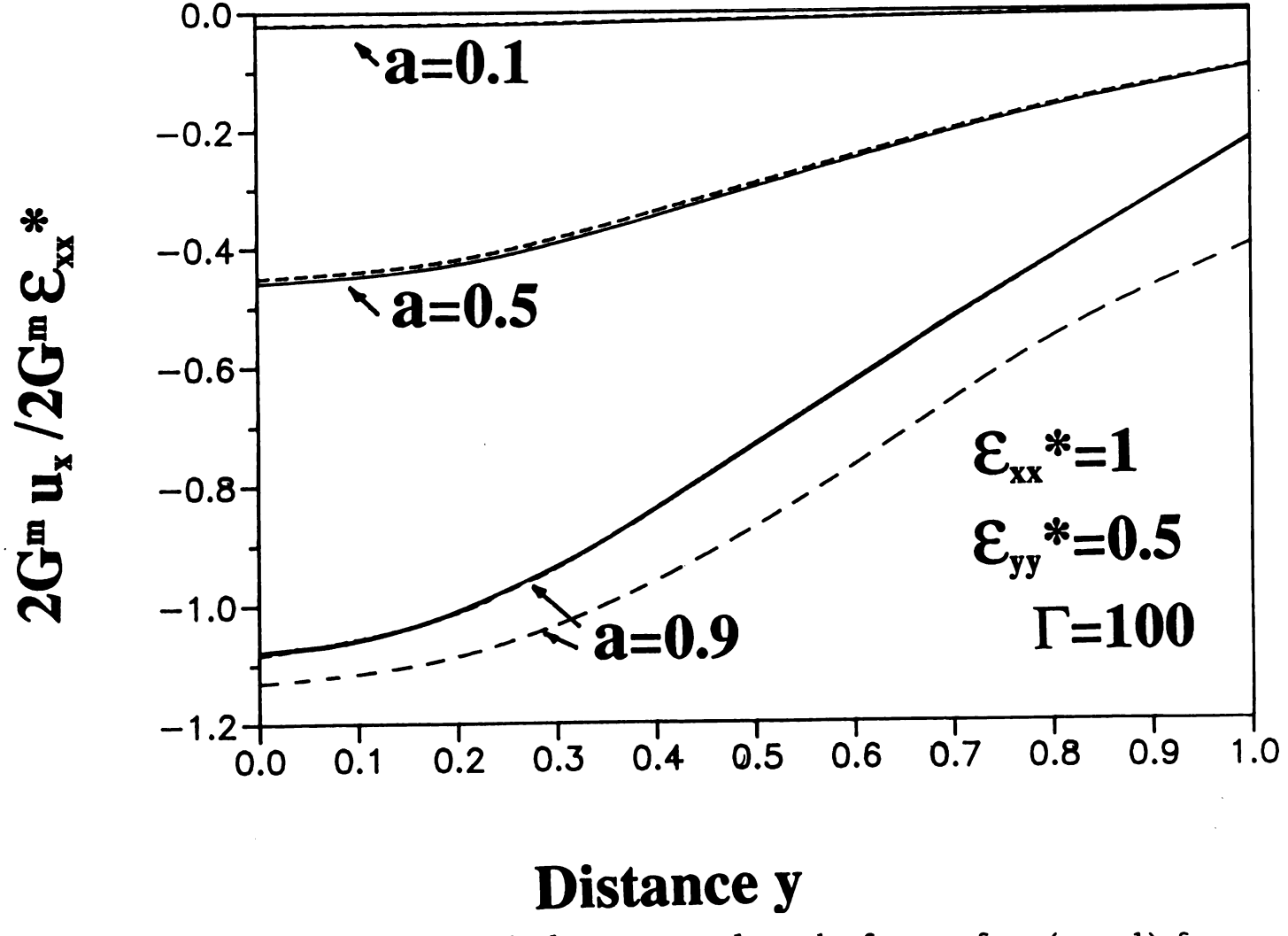

Fig. 17 Displacement u_x along the free surface (x = -1) for $\epsilon_{xx}^* = \epsilon_{zz}^* = 2\,\epsilon_{yy}^*$ for an infinite strip case when $\Gamma = 100$.

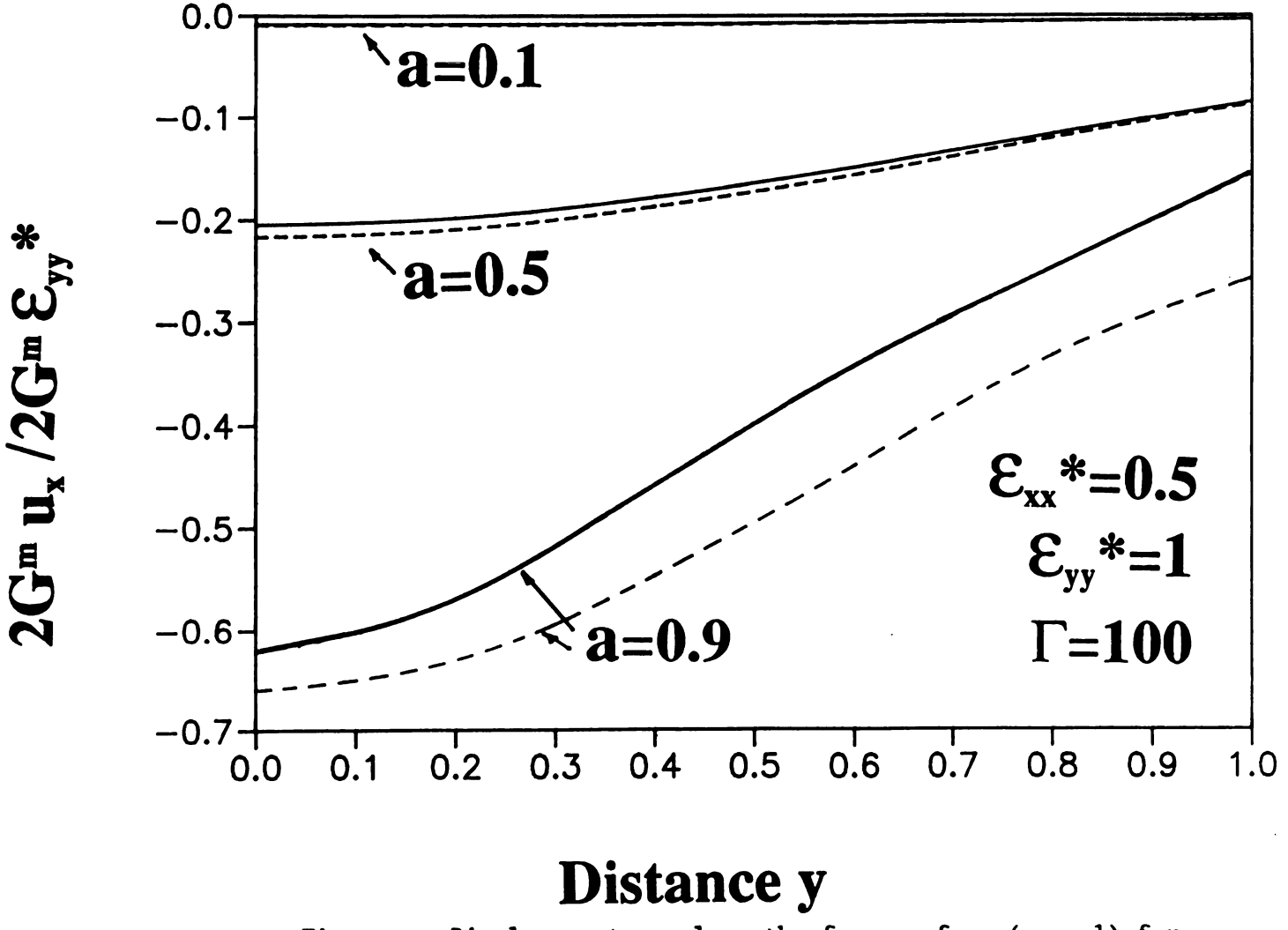

Fig. 18 Displacement u_x along the free surface (x = -1) for $\epsilon_{yy}^* = \epsilon_{zz}^* = 2\,\epsilon_{xx}^*$ for an infinite strip case

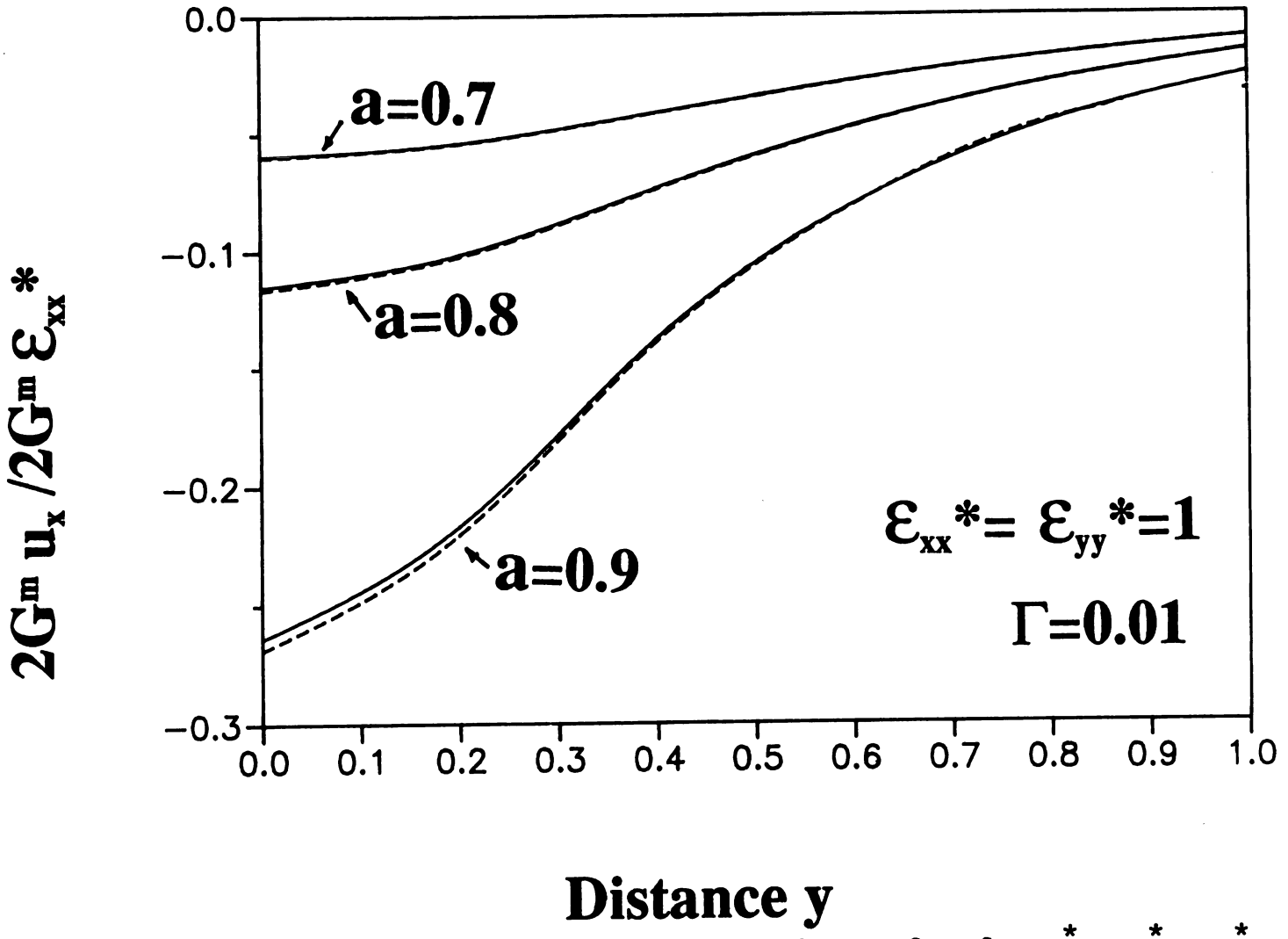

Fig. 19 Displacement u_x along the free surface for $\epsilon_{xx}^* = \epsilon_{yy}^* = \epsilon_{zz}^*$ for an infinite strip when $\Gamma = 0.01$. ($x = -1$)

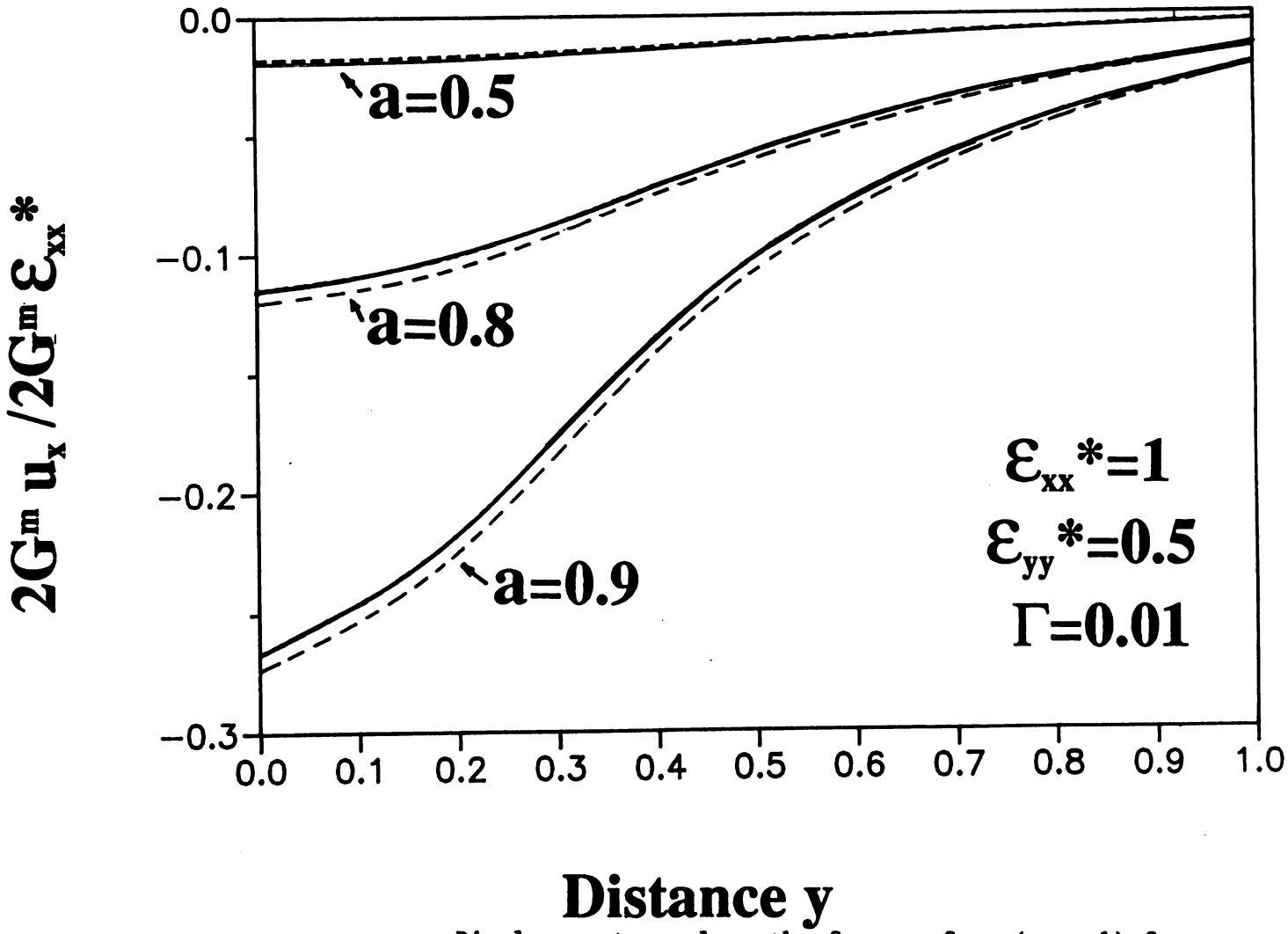

Fig. 20 Displacement u_x along the free surface (x = -1) for $\epsilon_{xx}^* = \epsilon_{zz}^* = 2\,\epsilon_{yy}^*$ for an infinite strip case when $\Gamma = 0.01$.

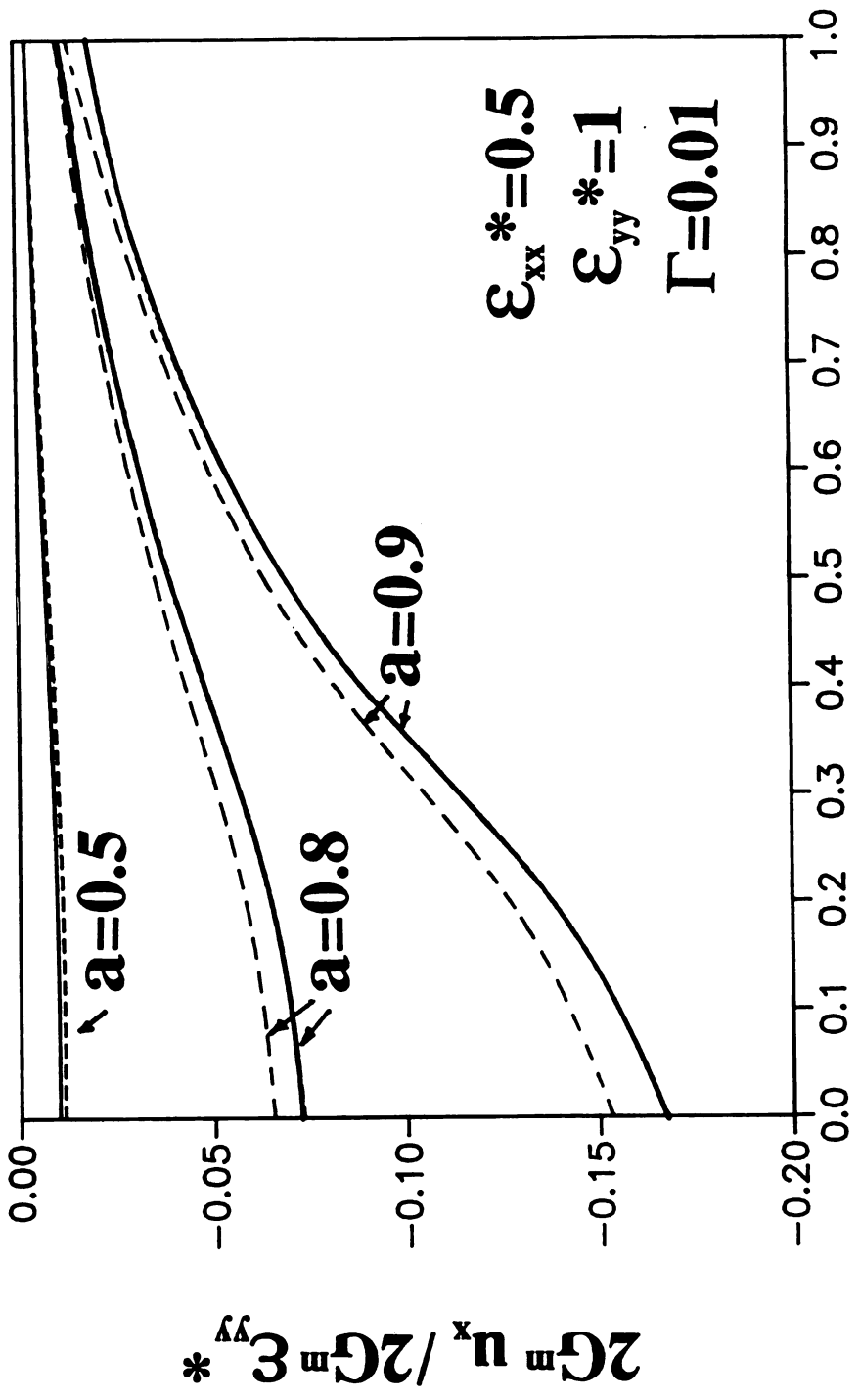

Fig. 21 Displacement u_x along the free surface (x = -1) for $\epsilon_{yy}^* = \epsilon_{zz}^* = 2\,\epsilon_{xx}^*$ for an infinite strip case when Γ = 0.01.

CHAPTER 4 : A Semi-Infinite Bimaterial Strip

INTRODUCTION

In the last part of this dissertation, the two dimensional elasticity problem of perfectly bonded semi-infinite bimaterial strips that are subjected to a constant temperature change is also considered. Physically, this geometry may represent a bimaterial thermostat used in electronic packaging. The strips are assumed to be linearly elastic and isotropic, and have different elastic and thermal properties.

We follow the procedure used by Bogy (1968), Blanchard and Ghoniem (1989) and Kuo (1989). We employ the Airy stress function approach along with Mellin transform and apply the residue theorem to the inversion integral in order to solve for the stress field at the interface when the two bonded quarter planes are subjected to a constant temperature change. Then this result is transformed by using the function $z = f(\zeta)$ defining the Schwarz-Christoffel transformation. This transformation maps the configuration of two quarter planes into the desired geometry of two semi-infinite strips. In order to satisfy the traction free boundary conditions we employ the iterative process used by Kuo (1989). Then the asymptotic behavior of stresses near the edge at the interface of two perfectly bonded strips is obtained.

METHOD OF SOLUTION

Consider the elasticity solution for the problem when the two perfectly bonded semi-infinite strips are subjected to a constant temperature change. In the notation used, the upper strip is denoted by double prime, while the lower strip is described by single prime. The problem considered is the plane elasticity problem. The solution is formulated in terms of polar coordinates.

1. Solution for the two elastic bonded quarter planes

Initially, we solve the problem of two perfectly bonded quarter planes (see Fig. 22). The method of solution for this part follows the papers by Bogy (1968) and Blanchard and Ghoniem (1989). We use the Airy stress function method. The governing equation is:

$$\nabla^4 \phi = 0 \tag{4.1}$$

The boundary conditions for the problem of two perfectly bonded quarter planes are given as follows:

a) the traction free conditions:

$$\begin{aligned} \sigma_{\theta\theta}' - \sigma_{r\theta}' &= 0 \qquad \text{at } \theta = -\frac{\pi}{2} \\ \sigma_{\theta\theta}'' - \sigma_{r\theta}'' &= 0 \qquad \text{at } \theta = +\frac{\pi}{2} \end{aligned} \tag{4.2}$$

b) the continuity conditions at the interface ($\theta = 0$):

$$\sigma_{\theta\theta}' = \sigma_{\theta\theta}''$$

$$\begin{aligned} \sigma_{r\theta}' &= \sigma_{r\theta}'' \\ u_r' &= u_r'' \\ u_\theta' &= u_\theta'' \end{aligned} \tag{4.3}$$

Next, we use Mellin transforms (Titchmarsh, 1948; Tranter, 1966) to simplify the solution process. The transforms for ϕ, σ_{ij} and u_i are defined as:

$$\begin{aligned} \hat{\phi}(s,\theta) &= \int_0^\infty \phi(r,\theta)\, r^{s-1} dr \\ \hat{\sigma}_{ij}(s,\theta) &= \int_0^\infty \sigma_{ij}(r,\theta) r^{s+1} dr \\ \hat{u}_i(s,\theta) &= \int_0^\infty u_i(r,\theta) r^s dr \end{aligned} \tag{4.4}$$

The governing differential equation (4.1) is transformed to:

$$\frac{d^4\hat{\phi}}{d\theta^4} + [(s+2)^2 + s^2] \frac{d^2\hat{\phi}}{d\theta^2} + s^2(s+2)^2\hat{\phi} = 0 \tag{4.5}$$

and the solution $\hat{\phi}$ is given as:

$$\hat{\phi}(s,\theta) = A\, e^{is\theta} + \bar{A}\, e^{-is\theta} + Be^{i(s+2)\theta} + \bar{B}\, e^{-i(s+2)\theta} \tag{4.6}$$

The expressions for the transformed stresses and displacements in terms of $\hat{\phi}$ are:

$$\begin{aligned} \hat{\sigma}_{r\theta}(s,\theta) &= (s+1)\frac{d\hat{\phi}}{d\theta} \\ \hat{\sigma}_{\theta\theta}(s,\theta) &= (s+1)\hat{\phi} \end{aligned} \tag{4.7}$$

$$\hat{u}_r(s,\theta) = \frac{1}{2\mu(s+1)} \{s(1+s - \frac{ms}{4}) \hat{\phi}(s,\theta) - \frac{m}{4} \frac{d^2}{d\theta^2} \hat{\phi}(s,\theta)\} - \frac{mT}{8\mu(s+1)}$$

$$\hat{u}_\theta(s,\theta) = \frac{1}{2\mu(s+1)(s+2)} \{[s+s^2 - \frac{ms^2}{4} - 2(s+1)^2] \frac{d}{d\theta} \hat{\phi}(s,\theta) -$$

$$\frac{m}{4} \frac{d^3}{d\theta^3} \hat{\phi}(s,\theta)\}$$

where

$$m = \begin{cases} \frac{4}{1+\nu} & \text{for plane stress} \\ 4(1-\nu) & \text{for plane strain,} \end{cases} \tag{4.8}$$

and

$$T = n E \alpha \Delta T \tag{4.9}$$

and μ, E, α, and ν are the shear modulus, Young's modulus, the coefficient of thermal expansion, and Poisson's ratio, respectively, and

$$n = \begin{cases} 1 & \text{for plane stress} \\ 1+\nu & \text{for plane strain} \end{cases} \tag{4.10}$$

The quantities, given in (4.7), are substituted in the boundary conditions (4.2)-(4.3). The traction free condition $\hat{\sigma}'_{r\theta} + i \hat{\sigma}'_{\theta\theta} = 0$ at $\theta = -\frac{\pi}{2}$ leads to

$$A' = \frac{1}{s} [B'(s+1) - \bar{B}' e^{is\pi}] \tag{4.11}$$

and the condition $\hat{\sigma}_{r\theta}'' + i\,\hat{\sigma}_{\theta\theta}'' = 0$ at $\theta = +\frac{\pi}{2}$ gives

$$A'' = \frac{1}{s}\,[B''(s+1) - \bar{B}''\, e^{-is\pi}] \tag{4.12}$$

It is convenient to rewrite the constants B', B'', $\bar{B}'$ and $\bar{B}''$ in terms of real and imaginary components:

$$\begin{aligned} B' &= 2E + 2Fi \qquad & B'' &= 2G + 2Hi \\ \bar{B}' &= 2E - 2Fi \qquad & \bar{B}'' &= 2G - 2Hi \end{aligned} \tag{4.13}$$

Using the relations (4.13), the continuity conditions at $\theta = 0$:

i) $\hat{u}_\theta'(s,0) = \hat{u}_\theta''(s,0)$ gives

$$\eta E + (\lambda - m')F + k\eta G + k(-\lambda + m'')H = 0 \tag{4.14}$$

where

$$k = \mu'/\mu'', \quad \xi = \frac{s\pi}{2}, \quad \eta = -\sin s\pi, \quad \lambda = 2s + 2 + 2\cos^2\xi$$

ii) $\hat{u}_r'(s,0) = \hat{u}_r''(s,0)$ yields

$$(\gamma + m')\,E + \eta F + k(-\gamma - m'')\,G + k\,\eta\,H = \frac{m'T' - \kappa m''T''}{16(s+1)} \tag{4.15}$$

where

$$\gamma = 2s + 2 - 2\cos^2\xi$$

iii) $\hat{\sigma}_{r\theta}' + i\hat{\sigma}_{\theta\theta}' = \hat{\sigma}_{r\theta}'' + i\,\hat{\sigma}_{\theta\theta}''$ gives

$$-\eta E - \lambda F - \eta G + \lambda H = 0 \tag{4.16}$$

$$\gamma E + \eta F - \gamma G + \eta H = 0 \tag{4.17}$$

Combining equations (4.14)-(4.17), the following system of four simultaneous linear equations is obtained:

$$\begin{bmatrix} \gamma & \eta & -\gamma & \eta \\ \eta & \lambda & \eta & -\lambda \\ \gamma+m & \eta & -k(\gamma+m') & k\eta \\ \eta & \lambda-m' & k\eta & -k(\lambda-m") \end{bmatrix} \begin{bmatrix} E \\ F \\ G \\ H \end{bmatrix} = \begin{bmatrix} 0 \\ 0 \\ \frac{m'T'-km"T}{16(s+1)} \\ 0 \end{bmatrix} \tag{4.18}$$

The determinant of the above matrix is given by

$$\|X\| = k_3^2\,\eta^2 + (k-1)^2(\gamma\lambda - \eta^2)^2 - k_2^2\,\gamma\lambda + k_2(k-1)(\lambda-\gamma)(\gamma\lambda - \eta^2) \tag{4.19}$$

where

$$k_2 = km" - m', \quad k_3 = km" + m' \tag{4.20}$$

The solution for the unknown constants E, F, G and H is

$$E = [\gamma\lambda\, k_2 + \eta^2\, k_3 + (k-1)\,\lambda\,(\eta^2 - \gamma\lambda)] \left[\frac{m'T'-km"T"}{16(s+1)}\right] \frac{1}{\|X\|}$$

$$F = [\eta(\gamma\lambda-\eta^2)(k-1) - 2k\gamma\eta m"] \left[\frac{m'T'-km"T"}{16(s+1)}\right] \frac{1}{\|X\|} \tag{4.21}$$

$$H = [\eta(k-1)(\eta^2-\gamma\lambda) - 2\gamma\eta m'] \left[\frac{m'T'-km"T"}{16(s+1)}\right] \frac{1}{\|X\|}$$

$$G = [-\eta^2 k_3 + \gamma\lambda k_2 + (k-1)\lambda(\eta^2-\gamma\lambda)]\left[\frac{m'T'-km''T''}{16(s+1)}\right]\frac{1}{\|X\|}$$

Therefore, using equations (4.6), (4.7), (4.11)-(4.13) and (4.21), the transformed stresses at the interface ($\theta = 0$) are given as:

$$\hat{\sigma}'_{r\theta}(s,0) = -F\,8(s+1)^2 + E\,4(s+1)\sin s\pi - F\,4(s+1)(\cos s\pi + 1)$$

$$\hat{\sigma}'_{\theta\theta}(s,0) = E\,8(s+1)^2 - E\,4(s+1)(\cos s\pi + 1)\,F - 4(s+1)\sin s\pi \tag{4.22}$$

$$\hat{\sigma}''_{r\theta}(s,0) = -H\,8(s+1)^2 - H\,4(s+1)(\cos s\pi + 1) - G\,4(s+1)\sin s\pi$$

$$\hat{\sigma}''_{\theta\theta}(s,0) = G\,8(s+1)^2 - G\,4(s+1)(\cos s\pi + 1) + H\,4(s+1)\sin s\pi$$

To recover the stresses in the real space we use Mellin's inversion integral (Titchmarsh, 1948) defined as

$$\sigma_{ij}(r,\theta) = \frac{1}{2\pi i}\int_{c-i\infty}^{c+i\infty} \hat{\sigma}_{ij}(s,\theta)r^{-(s+2)}ds \tag{4.23}$$

We perform the contour integration of (4.23) by using Cauchy's residue theorem (Marshen, 1973) and we obtain

$$\sigma_{ij}(r,\theta) = \lim_{s\to s_1}[(s-s_1)\,\hat{\sigma}_{ij}(s,\theta)r^{-(s+2)}] \tag{4.24}$$

where s_1 is the root of the determinant $\|X\|$ and it depends on the combination of elastic constants.

Using (4.24), the stresses at the interface are given as

$$\sigma'_{r\theta}(r,\theta)_{\theta=0} = \sigma''_{r\theta}(r,\theta)_{\theta=0} = [-(2s + 3 + \cos s\pi)\{\eta(\gamma\lambda - \eta^2)(k-1) - 2k\gamma\eta m''\} + \{\gamma\lambda k_2 + \eta^2 k_3 + \lambda(k-1)(\eta^2 - \gamma\lambda)\}\sin s\pi]_{s=s_1}$$

$$\frac{\Delta T}{4\frac{d}{ds}\|X\|_{s=s_1}} r^{-(s_1+2)} [n' m' E' \alpha' - k n'' m'' E'' \alpha'']$$

$$\sigma'_{\theta\theta}(r,\theta)_{\theta=0} = \sigma''_{\theta\theta}(r,\theta)_{\theta=0} = [(2s + 1 - \cos s\pi)\{\lambda(\eta^2 - \gamma\lambda)(k-1) + \gamma\lambda k_2 + \eta^2 k_3\} + \{(k-1)(\eta^3 - \eta\gamma\lambda) + 2k\gamma\eta m''\}\sin s\pi]_{s=s_1}$$

$$\frac{\Delta T}{4\frac{d}{ds}\|X\|_{s=s_1}} r^{-(s_1+2)} [n' m' E' \alpha' - k n'' m'' E'' \alpha''] \qquad (4.25)$$

$$\sigma'_{rr}(r,\theta)_{\theta=0} = [-(2s + 5 - \cos s\pi)\{\gamma\lambda k_2 + \eta^2 k_3 + (k-1)(\lambda\eta^2 - \gamma\lambda^2)\} + \sin s\pi\{(\eta\gamma\lambda - \eta^3)(k-1) - 2k\gamma\eta m''\}]_{s=s_1}$$

$$\frac{\Delta T}{4\frac{d}{ds}\|X\|_{s=s_1}} r^{-(s_1+2)} [n' m' E' \alpha' - k n'' m'' E'' \alpha'']$$

$$\sigma''_{rr}(r,\theta)_{\theta=0} = [-(2s + 5 - \cos s\pi)\{-\eta^2 k_3 + \gamma\lambda k_2 + (k-1)(\lambda\eta^2 - \gamma\lambda^2)\} + \sin s\pi\{(k-1)(\gamma\lambda\eta - \eta^3) + 2\gamma\eta m'\}]_{s=s_1}$$

$$\frac{\Delta T}{4\frac{d}{ds}\|X\|_{s=s_1}} r^{-(s_1+2)} [n' m' E' \alpha' - k n'' m'' E'' \alpha'']$$

Note that the stresses at the interface, given in (4.25), are of form:

$$\sigma_{ij}(r,\theta)_{\theta=0} = C_{ij} r^{-(s_1+2)} \qquad (4.26)$$

Recall that s_1 is the root of the determinant (4.19), which lies in the interval $-2 < s_1 < -1$. It is shown by Bogy (1968), that when $k_2[4(k-1)-k_2] > 0$, there exists one real root in that interval. This case will give us the algebraic singularity of form $r^{-\lambda}$. This situation is of

interest in this paper. In general, the problems of this nature could have stresses of forms $r^{-\lambda}$, r^0 or ln r. For the more complete discussion on this topic see papers by Bogy (1968, 1970), Dundurs (1969), and Blanchard and Ghoniem (1989).

2. Solution for the two elastic bonded semi-infinite strips

Next, we want to use the solution of two quarter planes to obtain the desired solution for the two semi-infinite strips. To accomplish this we use a conformal mapping (Nehari, 1952). The Schwarz-Christoffel transformation for mapping the half-plane (Re(z)>0) into the interior of semi-infinite strip ($-h_1<\mathrm{Re}(\zeta)<h_2$, $\mathrm{Im}(\zeta)>0$), as seen in Fig. 22, is derived as

$$\zeta = \alpha \int_0^{iz} \frac{dz}{\sqrt{1-z^2}} = \alpha \sin^{-1} iz + \beta \tag{4.27}$$

The constants α and β are determined by using

$$\begin{aligned} \zeta &= -h_1, \quad z = +i \\ \zeta &= +h_2, \quad z = -i \end{aligned} \tag{4.28}$$

Therefore,

$$z = -i \sin\left\{ \frac{\pi}{h_1+h_2} \left(\zeta + \frac{h_1-h_2}{2}\right)\right\} = \omega(\zeta) \tag{4.29}$$

where $z = r\, e^{i\theta}$ and $\zeta = \rho\, e^{i\phi}$.

Next, we use the relations between the original and transformed stresses (Muskhelishvili, 1953)

$$\sigma_{\rho\rho} + \sigma_{\phi\phi} = \sigma_{rr} + \sigma_{\theta\theta} \tag{4.30}$$

$$\sigma_{\phi\phi} - \sigma_{\rho\rho} + 2i\,\sigma_{\rho\phi} = (\sigma_{\theta\theta} - \sigma_{rr} + 2i\,\sigma_{r\theta})\, e^{2i\alpha}$$

where

$$e^{2i\alpha} = \frac{\zeta^2}{\rho^2} \frac{\omega'(\zeta)}{\bar{\omega}'(\zeta)} \tag{4.31}$$

Using (4.29),

$$\omega'(\zeta) = \frac{d\omega}{d\zeta} = \frac{-\pi i}{h_1+h_2} \cos\{\frac{\pi}{h_1+h_2}(\zeta + \frac{h_1-h_2}{2})\} \tag{4.32}$$

and

$$\bar{\omega}'(\zeta) = \frac{\pi i}{h_1+h_2} \cos\{\frac{\pi}{h_1+h_2}(\bar{\zeta} + \frac{h_1-h_2}{2})\} \tag{4.33}$$

equation (4.31) becomes

$$e^{2i\alpha} = \frac{\zeta^2}{\rho^2} (-1) \frac{\cos\{ \frac{\pi}{h_1+h_2} (\zeta + \frac{h_1-h_2}{2})\}}{\cos\{ \frac{\pi}{h_1+h_2} (\bar{\zeta} + \frac{h_1-h_2}{2})\}} \tag{4.34}$$

At the interface of the two semi-infinite strips, where $\phi = \frac{\pi}{2}$, for the case of $h_1 = h_2 = h$, equation (4.34) reduces to

$$e^{2i\alpha} = 1 \tag{4.35}$$

Therefore, the relations (4.30) become

$$\sigma_{\rho\rho} + \sigma_{\phi\phi} = \sigma_{rr} + \sigma_{\theta\theta} \tag{4.36}$$

$$\sigma_{\phi\phi} - \sigma_{\rho\rho} + 2i\sigma_{\rho\phi} = \sigma_{\theta\theta} - \sigma_{rr} + 2i\sigma_{r\theta}$$

Also, at the interface where $\phi = \frac{\pi}{2}$

$$r = -i \sin\left(\frac{\pi\rho}{2h}\, i\right) = -\, i^2 \sinh\left(\frac{\pi\rho}{2h}\right) = \sinh\left(\frac{\pi\rho}{2h}\right) \tag{4.37}$$

Therefore, the stresses at the interface of the two semi-infinite elastic strips are:

$$\sigma'_{\rho\phi}\left(\rho,\frac{\pi}{2}\right) = (n'm'E'\alpha' - k\, n''m''E''\alpha'')[\gamma\lambda\eta(2km'' - k_2) - \eta^2 k_3]_{s=s_1}$$
$$\frac{\Delta T}{4\,\frac{d}{ds}\|X\|_{s=s_1}} \sinh\left[\frac{\pi\rho}{2h}\right]^{-(s_1+2)} \tag{4.38}$$

$$\sigma''_{\rho\phi}\left(\rho,\frac{\pi}{2}\right) = (n'm'E'\alpha' - k\, n''m''E''\alpha'')[\gamma\lambda\eta(2m' + k_2) - \eta^2 k_3]_{s=s_1}$$
$$\frac{\Delta T}{4\,\frac{d}{ds}\|X\|_{s=s_1}} \sinh\left[\frac{\pi\rho}{2h}\right]^{-(s_1+2)} \tag{4.39}$$

$$\sigma'_{\phi\phi}\left(\rho,\frac{\pi}{2}\right) = (n'm'E'\alpha' - k\, n''m''E''\alpha'')[2\eta^2\gamma\lambda(k-1) - \gamma^2\lambda^2(k-1)$$
$$+ \gamma^2\lambda k_2 + \gamma\eta^2 k_3 - \eta^4(k-1) - 2\gamma\eta^2(k_3 + m')]_{s=s_1}$$
$$\frac{\Delta T}{4\,\frac{d}{ds}\|X\|_{s=s_1}} \sinh\left[\frac{\pi\rho}{2h}\right]^{-(s_1+2)} \tag{4.40}$$

$$\sigma''_{\phi\phi}\left(\rho,\frac{\pi}{2}\right) = (n'm'E'\alpha' - k\, n''m''E''\alpha'')[2\eta^2\gamma\lambda(k-1) - \gamma^2\lambda^2(k-1) + \gamma^2\lambda k_2$$

$$- \gamma\eta^2 k_3 - \eta^4(k-1) + 2\gamma\eta^2 m']_{s=s_1} \frac{\Delta T}{4 \frac{d}{ds} \|X\|_{s=s_1}} \sinh\left[\frac{\pi\rho}{2h}\right]^{-(s_1+2)} \tag{4.41}$$

$$\sigma_{\rho\rho}'(\rho,\tfrac{\pi}{2}) = (n'm'E'\alpha' - k\, n''m''E''\alpha'')[(-2s-5+\cos s\pi)\{\gamma\lambda k_2+\eta^2 k_3 + (k-1)(\lambda\eta^2 - \gamma\lambda^2)\} + \sin s\pi\{(\eta\gamma\lambda - \eta^3)(k-1) - 2k\gamma\eta m''\}]_{s=s_1} \frac{\Delta T}{\frac{d}{ds}\|X\|_{s=s_1}} \sinh\left[\frac{\pi\rho}{2h}\right]^{-(s_1+2)} \tag{4.42}$$

$$\sigma_{\rho\rho}''(\rho,\tfrac{\pi}{2}) = (n'm'E'\alpha' - k\, n''m''E''\alpha'')[(-2s-5+\cos s\pi)\{-\eta^2 k_3 + \gamma\lambda k_2 + (k-1)(\eta^2\lambda - \gamma\lambda^2)\} + \sin s\pi\{(k-1)(\gamma\eta\lambda - \eta^3) + 2\gamma\eta m'\}]_{s=s_1} \frac{\Delta T}{4\frac{d}{ds}\|X\|_{s=s_1}} \sinh\left[\frac{\pi\rho}{2h}\right]^{-(s_1+2)} \tag{4.43}$$

Clearly, the shearing stresses in (4.38)-(4.39) and peeling stresses in (4.40)-(4.41) satisfy continuity conditions at the interface.

So, the stresses at the interface of the two semi-infinite strips, given in (4.38)-(4.43), are of form

$$\sigma_{ij}(\rho,\tfrac{\pi}{2}) = C_{ij} \sinh\left[\frac{\pi\rho}{2h}\right]^{-(s_1+2)} \tag{4.44}$$

When $\rho \to 0$,

$$\sinh\left[\frac{\pi\rho}{2h}\right] \approx \frac{\pi\rho}{2h} \tag{4.45}$$

Therefore, the stresses are expressed as

$$\sigma_{ij}(\rho,\tfrac{\pi}{2}) = C_{ij}\left(\frac{\rho}{h}\right)^{-(s_1+2)} \tag{4.46}$$

Again, when $-2 < s_1 < -1$, the stresses are singular as $\rho \to 0$.

After the transformation of shape from two quarter planes to two semi-infinite strips we need to check the tractions on the boundary (see Fig. 22):

a) at $v = 0$ and $-h \le u \le 0$, $e^{2i\alpha} = -1$. Therefore,

$$\sigma''_{uv} = 0,\ \sigma''_{uu} = \sigma''_{yy},\ \sigma''_{vv} = 0 \tag{4.47}$$

b) at $v = 0$ and $0 \le u \le h$, $e^{2i\alpha} = -1$

$$\sigma'_{uv} = 0,\ \sigma'_{uu} = \sigma'_{yy},\ \sigma'_{vv} = 0 \tag{4.48}$$

c) at $u = -h$ and $v > 0$

$$\sigma''_{uv} = -\sigma''_{yy}\frac{hv}{h^2+v^2},\ \sigma''_{uu} = \sigma''_{yy}\frac{v^2}{h^2+v^2},\ \sigma''_{vv} = \sigma''_{yy}\frac{h^2}{h^2+v^2} \tag{4.49}$$

d) at $u = h$ and $v > 0$

$$\sigma'_{uv} = \sigma'_{yy}\frac{hv}{h^2+v^2},\ \sigma'_{uu} = \sigma'_{yy}\frac{v^2}{h^2+v^2},\ \sigma'_{vv} = \sigma'_{yy}\frac{h^2}{h^2+v^2} \tag{4.50}$$

The stresses on the lateral surfaces, given in equations (4.49)-(4.50), do not vanish, as specified by traction free boundary conditions. Therefore, we need to cancel these tractions by applying the additional loading. Therefore, these additional stresses are, at $u = -h$,

$$\sigma''_{uv} = - C_{II} \frac{(\cosh \frac{\pi v}{2h})^{-(s_1+2)} hv}{h^2 + v^2} ,$$

$$\sigma''_{uu} = C_{II} \frac{(\cosh \frac{\pi v}{2h})^{-(s_1+2)} v^2}{h^2 + v^2} \tag{4.51}$$

and at u = h

$$\sigma'_{uv} = C_I \frac{(\cosh \frac{\pi v}{2h})^{-(s_1+2)} hv}{h^2 + v^2} ,$$

$$\sigma'_{uu} = C_I \frac{(\cosh \frac{\pi v}{2h})^{-(s_1+2)} v^2}{h^2 + v^2} \tag{4.52}$$

where

$$C_I = \{-A[s \cos\frac{s\pi}{2} + (s+4)\cos\frac{(s+2)\pi}{2}] - B[-s \sin\frac{s\pi}{2} + (s+4) \sin\frac{(s+2)\pi}{2}]\}_{s=s_1}$$

$$\frac{m' T' - km'' T''}{4 \frac{d}{ds} \|X\|_{s=s_1}} \tag{4.53}$$

$$C_{II} = \{-C[s \cos\frac{s\pi}{2} + (s+4)\cos\frac{(s+2)\pi}{2}] - D[-s \sin\frac{s\pi}{2} + (s+4) \sin\frac{(s+2)\pi}{2}]\}_{s=s_1}$$

$$\frac{m' T' - km'' T''}{4 \frac{d}{ds} \|X\|_{s=s_1}}$$

and

$$A = \gamma\lambda k_2 + \eta^2 k_3 + (k-1) \lambda (\eta^2 - \gamma\lambda)$$

$$B = \eta(\gamma\lambda-\eta^2)(k-1) - 2k\gamma\eta m''$$

$$C = \eta(k-1)(\eta^2-\gamma\lambda) - 2\gamma\eta m' \qquad (4.54)$$

$$D = -\eta^2 k_3 + \gamma\lambda k_2 + (k-1)\lambda(\eta^2-\gamma\lambda)$$

3. Iteration procedure for the boundary adjustment

For the remaining part of the solution we follow Kuo's (1989) paper (sections 4 and 5). Initially, we solve the problem of two infinite strips with the loading given in equations (4.51)-(4.52), but of the opposite sign. Superposing this solution with the previous solution of semi-infinite strips we could have normal tractions at the transverse edge. These tractions need to be cancelled. So the additional problem of the two quarter planes subjected to normal tractions needs to be solved. In this step we follow solution of Bogy (1970). This loading in turn gives rise to the additional lateral tractions which need to be cancelled. This procedure will be repeated until it satisfies the convergence criterion. The details of this iteration procedure are given in Kuo's paper and are not repeated here.

For the numerical example considered in this paper, the iteration procedure is done only once. The remaining tractions on the lateral surface are very small and their contribution to the stresses along the interface is negligible.

RESULTS AND DISCUSSION

In the numerical example we consider a thermostat having the following properties:

Aluminum	Molybdenum
$\nu'' = 0.345$	$\nu' = 0.293$
$E'' = 70380$ MPa	$E' = 325000$ MPa
$\alpha'' = 23.6 \times 10^{-6}/^{0}C$	$\alpha' = 4.9 \times 10^{-6}/^{0}C$

We solve the case when the thickness is much smaller than the other dimensions. Therefore, we have plane stress case. We take $h_1 = h_2 = h$. The stress distribution at the interface of the semi-infinite bimetallic molybdenum/aluminum strip is illustrated in Fig. 23. In the discussion we assume that the temperature change $\Delta T > 0$. Note that the axial stress, $\sigma''_{\rho\rho}$, in the aluminum strip is compressive and $\sigma'_{\rho\rho}$ in the molybdenum strip is tensile, as expected, since the thermal expansion coefficients $\alpha'' > \alpha'$. The peeling stress $\sigma''_{\phi\phi} = \sigma'_{\phi\phi}$ is compressive along the interface. Kuo (1989) solves the same thermostat problem. However, in his paper Figs. 4 and 5, which represent the axial stress, give the results that do not agree with ours. Also, we observe that he solves the problem of plane strain, although the plane stress case was supposed to be considered. Note, that the elasticity solution yields singular stresses at the edge at the interface of two strips. The singular term is of form $[\rho/h]^{-1/(s_1+2)}$. For the case of molybdenum/aluminum semi-infinite strips $s_1 = -1.8875$. The similar geometries such as two dissimilar quarter planes or wedges also yield singular stresses at the

interface near the edge or corner and the form of singularity depends on the combination of elastic constants, as shown by Bogy (1968, 1970), Dundurs (1969), Hein and Erdogan (1971), Dempsey and Sinclair (1981), and Blanchard and Ghoniem (1989), among others.

The problem of bimaterial thermostat has received considerable attention in literature because of its application in the electronic packaging industry. The different solution approaches to this problem give different stresses at the interface. For example, the elasticity solutions by Kuo (1989) and in this dissertation give the singular stresses at the edge at the interface as expected from theory of elasticity. The approximate methods based on strength of materials approach and energy methods do not give singular stresses at the edge at the interface. For example, Suhir (1989) imposes the condition of zero shear stress at the edge along the interface as suggested by Razaqpar (1987). There also exists a number of finite element solutions. However many of these solutions are incorrect as discussed by Lau (1989). The present result for the stresses at the interface at the edge is in agreement with the finite element solution of Lau (1989). In this dissertation we propose another solution for this very interesting and challenging problem. Our solution is singular as expected by theory of elasticity. In reality, however, the material cannot sustain infinite stresses, but the proper interpretation of these results may increase the understanding of the stress field. Also, our solution can give guidance to the researchers using finite element method regarding the nature of the elements to be employed.

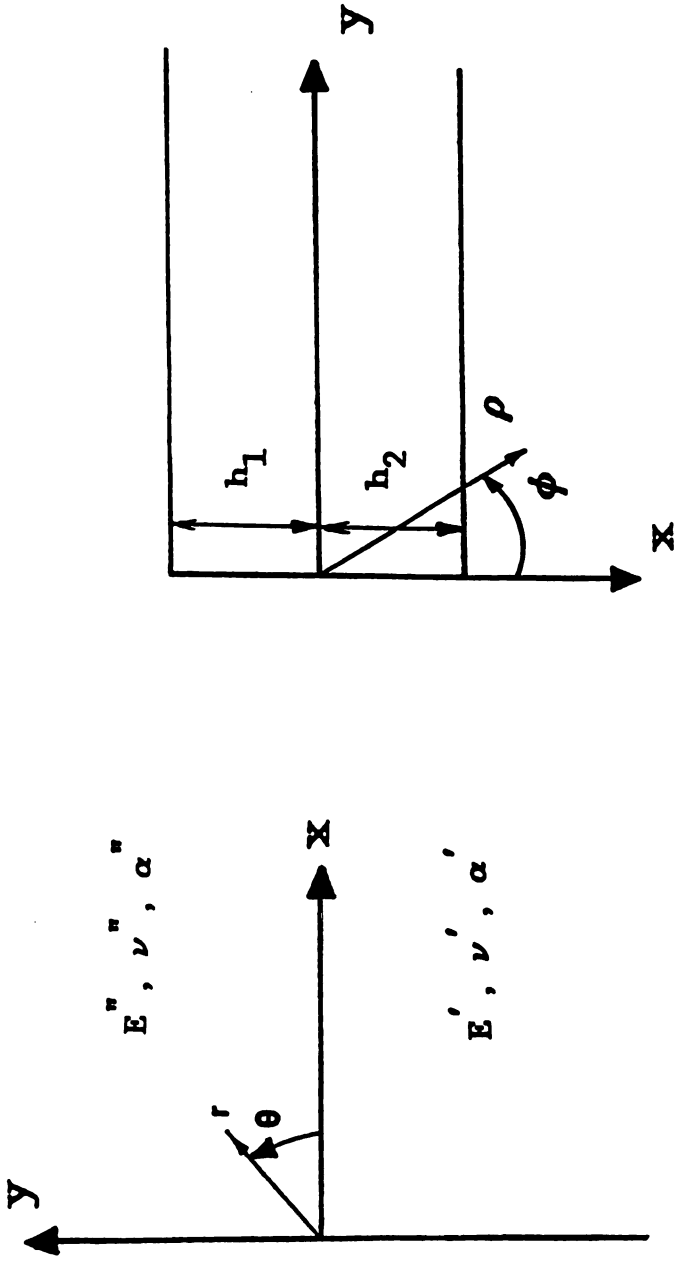

Fig. 22 Two quater planes and two semi-infinite strips.

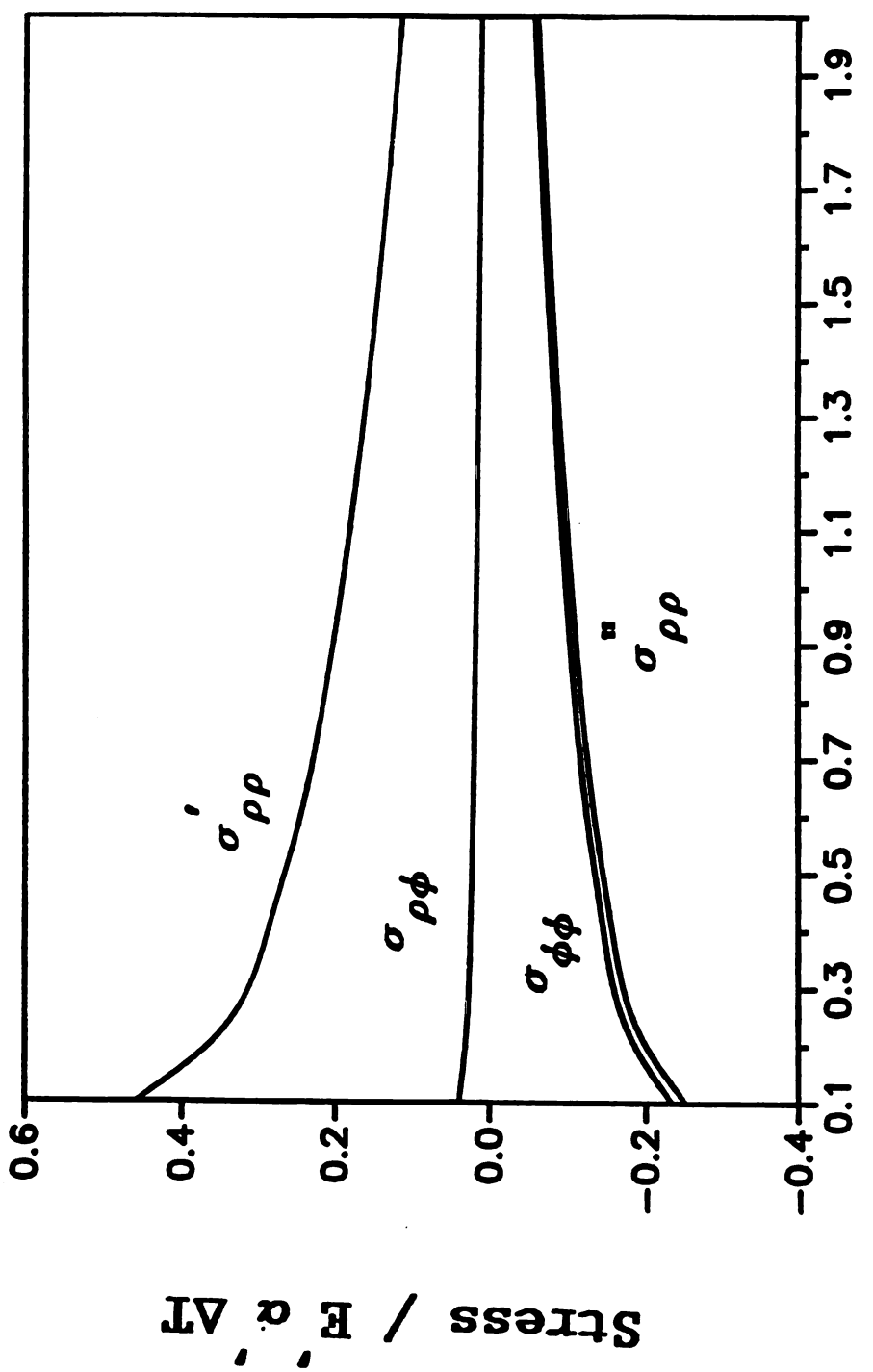

Fig. 23 Stresses at the interface of a bimetallic semi-infinite strip.

CHAPTER 5 : CONCLUSIONS

The plane elasticity problems of a semi-infinite bimaterial strip subjected to a temperature change and a circular inclusion in a half-plane and an infinite strip under thermo-mechanical loading have been investigated analytically. We used Papkovich-Neuber displacement potentials in an infinite series form and Airy stress functions, respectively.

The numerical examples illustrate how the joint effect of free surface, the mismatch of material constants, the geometry, the type of loadings, and the boundary conditions effect the stresses and displacements.

The study of the problem when an inclusion is embedded in a half plane or an infinite strip shows that the stiffer the inclusion (or the larger the Γ) the more pronounced is the effect of interface. The effect of free surface contributes significantly to the stress disturbance when the inclusion embedded close to the free surface (or surfaces). The stresses do actually increase locally due to the sliding boundary condition. The solution of the semi-infinite bimaterial strip gives the singular stresses at the interface at the edge of the strip.

REFERENCES

Aderogba, K., 1976, "On Eigenstresses in a Semi-infinite Solid," Mathematical Proceedings of the Cambridge Philosophical Society, Vol. 80, pp. 555-562.

Aleck, B. J., 1949, "Thermal Stresses in a Rectangular Plate Clamped along the Edge," ASME Journal of Applied Mechanics, Vol. 16, pp. 118-122.

Blanchard, J. P. and Ghoniem, N. M., 1989, "Relaxation of Thermal Stress Singularities in Bonded Viscoelastic Quarter Planes," ASME Journal of Applied Mechanics, Vol. 56, pp. 756-762.

Blech, J. J. and Kantor, Y., 1984, "An Edge Problem having no Singularity at the Corner," Computers and Structures, Vol. 18, pp. 609-617.

Bogy, D. B., 1970, "On the Problem of Edge-bonded Elastic Quarter Planes Loaded at the Boundary," International Journal of Solids and Structures, Vol. 6, pp. 1287-1313.

Bogy, D. B., 1968, "Edge-bonded Dissimilar Orthogonal Elastic Wedges under Normal and Shear Loading," ASME Journal of Applied Mechanics, Vol. 35, pp. 460-466.

Callias, C. J., and Markenscoff, X., 1989, "Singular Asymptotics Analysis for the Singularity at a Hole near a Boundary," Quarterly of Applied Mathematics, Vol. 47, pp. 233-245.

Chen, D., Cheng, S, and Gerhart, T. D., 1982, "Thermal Stresses in Laminated Beams, Journal of Thermal Stresses, Vol. 5, pp. 67-84.

Chen, W. T. and Nelson, C. W., 1979, "Thermal Stress in Bolted Joints," IBM Journal of Research and Development, Vol. 23, pp. 178-188.

Cox, B. N., Marshall, D. B., Kouris, D., and Mura, T., 1988, "Surface Displacement Analysis of the Transformed Zone in Magnesia Partially Stabilized Zirconia," ASME Journal of Engineering Materials and Technology, Vol. 110, pp. 105-109.

Dempsey, J.P. and Sinclair, G.B., 1981, "On the Singular Behavior at the Vertex of a Bi-material Wedge," Journal of Elasticity, Vol. 11, pp. 317-327.

Dundurs, J., 1969, discussion, ASME Journal of Applied Mechanics, Vol. 36, pp. 650-652.

Eischen, J. W., Chung, C. and Kim, J. H., 1990, "Realistic Modeling of Edge Effect Stresses in Bimaterial Elements," ASME Journal of Electronic Packaging, Vol. 112, pp. 16-23.

Eshelby, J. D., 1957, "The Determination of the Elastic Fields of an Ellipsoidal Inclusion, and Related Problems," Proceedings of Royal Society, London, Vol. A241, pp. 376-396.

Gerstle, F. P. and Chambers, R. S., 1987, "Analysis of End Stresses in Glass-Metal Bi-Material strips," in Technology of Glass, Ceramic or Glass-Ceramic to Metal Sealing, eds. W. E. Moddeman, C. W. Merten and D. P. Kramer, ASME, NY, pp. 47-59.

Hein, V. L. and Erdogan, F., 1971, "Stress Singularities in a Two-Material Wedge," International Journal of Fracture Mechanics, Vol. 7, pp. 317-330.

Hess, M. S., 1969, "The End Problem for a Laminated Elastic Strip- I. The General Solution," Journal of Composite Materials, Vol. 3, pp. 262-292.

Hess, M. S., 1969, "The End Problem for a Laminated Elastic Strip- II. Differential Expansion Stresses," Journal of Composite Materials, Vol. 3, pp. 630-641.

Howland, R.C.J., and Stevenson, A.C., 1933, "Bi-Harmonic Analysis in a Perforated Strip", Philosophical Transactions of the Royal Society of London, Series A, Vol. 232, pp. 155-222.

Hussain, M. A., and Pu, S. L., 1971, "Slip Phenomenon for a Circular Inclusion," ASME Journal of Applied Mechanics, Vol. 38, pp. 627-633.

Ishiwata, K., 1986, "Stress Concentration due to an Elliptic Hole or a Griffith Crack in a Semi-infinite Elastic Plate under Tension," Master's Dissertation, Saitama University, Japan.

Jasiuk, I., Tsuchida, E., and Mura, T., 1987, "The Sliding Inclusion Under Shear," International Journal of Solids and Structures, Vol. 23, pp. 1373-1385.

Jeffery, G. B., 1920, "Plane Stress and Plane Strain in Bipolar Coordinates," Transactions of Royal Society, London, Series A, Vol. 221, pp. 265-293.

Keer, L. M., Dundurs, J., and Kiattikomol, K., 1973, "Separation of a Smooth Circular Inclusion from a Matrix," International Journal of Engineering Science, Vol. 11, pp. 1221-1233.

Knight, R.C., 1934, "On the Stresses in a Perforated Strip," Quarterly Journal of Mathermatics, Vol. 5, pp. 255-278.

Kouris, D., and Mura, T., 1989, "The Elastic Field of a Hemispherical Inhomogeneity at the Free Surface of an Elastic Half Space," Journal of the Mechanics and Physics of Solids, Vol. 37, pp. 365-379.

Kouris, D., Tsuchida, E., and Mura, T., 1988, "An Anomaly of Sliding Inclusions," ASME Journal of Applied Mechanics, Vol. 53, pp. 724-726.

Kouris, D., Tsuchida, E., and Mura, T., 1989, "The Hemispheroidal Inhomogeneity at the Free Surface of an Elastic Half Space," ASME Journal of Applied Mechanics, Vol. 56, pp. 70-76.

Kuo, A.Y., 1989, "Thermal Stresses at the Edge of Bimetallic Thermostat," ASME Journal of Applied Mechanics, Vol. 56, pp. 585-589.

Lau, J. H., 1989, "A Note on the Calculation of Thermal Stresses in Electronic Packaging by Finite Element Methods," ASME Journal of Electronic Packaging, Vol. 111, pp. 313-320.

Margetson, J., and Morland, L. W., 1970, "Separation of Smooth Circular Inclusions from Elastic and Viscoelastic Plates Subjected to Uniaxial Tension," Journal of the Mechanics and Physics of Solids, Vol. 18, pp. 295-309.

Marsden, J. E., 1973, Basic Complex Analysis, Freeman and Co, San Francisco.

Mindlin, R. D., 1948, "Stress Distribution Around a Hole Near the Edge of a Plate Under Tension," Proceedings of the Society for Experimental Stress Analysis, Vol. 5, pp. 56-68.

Mindlin, R. D., and Cheng, D. H., 1950, "Thermoelastic Stress in the Semi-infinite Solid," Journal of Applied Physics, Vol. 21, pp. 931-933.

Mura, T., 1987, Micromechanics of Defects in Solids, 2nd ed., Martinus Nijhoff, Dordrecht.

Mura, T., 1985, "A new NDT: Evaluation of plastic strains in bulk from displacements on surfaces," Mechanics Research Communications, Vol. 12, pp. 243-248.

Mura, T., and Furuhashi, R., 1984, "The Elastic Inclusion With a Sliding Interface," ASME Journal of Applied Mechanics, Vol. 51, pp. 308-310.

Mura, T., Jasiuk, I., and Tsuchida, E., 1985, "The Stress Field of a Sliding Inclusion," International Journal of Solids and Structures, Vol. 21, pp. 1165-1179.

Muskhelishvili, N. I., 1953, Some Basic Problems of the Mathematical Theory of Elasticity, P. Noordhoff Ltd., Groningen, Holland, pp. 214-217.

Nehari, Z., 1952, Conformal Mapping, McGraw-Hill, Inc., New York.

Noble, B., and Hussain, M. A., 1969, "Exact Solution of Certain Dual Series for Indentation and Inclusion Problems," International Journal of Engineering Science, Vol. 7, pp. 1149-1161.

Razaqpar, A. G., 1987, Discussion on Suhir's paper (1986), ASME Journal of Applied Mechanics, Vol. 54, p. 479.

Reissner, E., 1947, "On bending of Elastic Plates," Quarterly of Applied Mathermatics, Vol. 5-6, pp. 55-68.

Richardson, M.K., 1969, "Interference Stresses in a Half Plane Containing an Elastic Disk of the Same Material," ASME Journal of Applied Mechanics, Vol. 36, pp. 128-130.

Saleme, E. M., 1958, "Stress Distribution Around a Circular Inclusion in a Semi-Infinite Elastic Plate," ASME Journal of Applied Mechanics, Vol. 25, pp. 129-135.

Seo, K., and Mura, T., 1979, "The Elastic Field in a Half-Space due to Ellipsoidal Inclusions with Uniform Dilatational Eigenstrains," ASME Journal of Applied Mechanics, Vol. 46, pp. 568-572.

Shioya, S., 1967, "On a Semi-Infinite Thin Plate with a Circular Inclusion under Uniform Tension," Bulletin of JSME, Vol. 10, pp. 1-9.

Stippes, M., Wilson, H. B., and Krull, F. N., 1962, "A Contact Stress Problem for a Smooth Disk in an Infinite Plate," Proceedings of the 4th U.S. National Congress of Applied Mechanics, ASME, pp. 799-806.

Suhir, E., 1989, "Interfacial Stresses in Bimetal Thermostats," ASME Journal of Applied Mechanics, Vol. 56, pp. 595-600.

Suhir, E., 1986, "Stress in Bi-metal Thermostat," ASME Journal of Applied Mechanics, Vol. 53, pp. 657-660.

Tamate, Osamu, 1956, "The Effect of a Circular Hole on the Pure Twest of an Infinite Strip", ASME Journal of Applied Mechanics, Vol. 23, pp. 115-121.

Theocaris, 1954, "The Stress Distribution in a Strip Loaded in Tension by Means of a Central Pin", ASME Journal of Applied Mechanics, Vol. 21, pp 85-90.

Tichtmarsh, E. C., 1948, Introduction to the Theory of Fourier Integrals, 2nd ed., Oxford Press, London.

Timoshenko, S., 1925, "Analysis of Bi-metal Thermostats," Journal of Optical Society of America, Vol. 11, pp. 595-600.

Tranter, C. J., 1966, Integral Transforms in Mathematical Physics, John Wiley & Sons, Inc., New York.

Tsuchida, E., and Yaegashi, A., 1981a, "The stresses in a Thick Plate Containing a Prolate Spheroidal Cavity Subjected to an Axisymmetric Pressure," Theoretical and Applied Mechanics, Vol. 31, pp. 85-96.

Tsuchida, E., and Yaegashi, A., 1981b, "The stresses in a Thick Plate Containing a Prolate Spheroidal Cavity Subjected to an Uniaxial Tension," JSME Bulletin, Vol. 25, pp. 411-420.

Tsuchida, E., and Mura, T., 1983, "The Stress Field in an Elastic Half-Space Having a Spheroidal Inhomogeneity Under All-Around Tension Parallel to the Plane Boundary," ASME Journal of Applied Mechanics, Vol. 50, pp. 807-816.

Tsuchida, E., Mura, T., and Dundurs, J., 1986, "The Elastic Field of an Elliptic Inclusion with a Slipping Interface," ASME Journal of Applied Mechanics, Vol. 53, pp. 103-107.

Tsuchida, E., Kouris, D., and Jasiuk, I., 1990, "The Hemispherical Inhomogeneity Subjected to a Concentrated Force," in Micromechanics and Inhomogeneity- The Toshio Mura 65th Aniversary Volume, eds. G.J. Weng, M. Taya and H. Abe, Springer-Verlag, New York, pp. 497-509.

Tsutsui, S., and Saito, K., 1973, "On the Effect of a Free Surface and a Spherical Inhomogeneity on Stress Fields of a Semi-Infinite Medium under Axisymmetric Tension," Proceedings of the 23rd Japan National Congress for Applied Mechanics, Vol. 23, pp. 547-560.

Wang, C., 1946, "Theoretical Analysis of Perforated Shear Webs", ASME Journal of Applied Mechanics, Vol. 13, pp. A-77-A-82.

APPENDIX

The displacements and stresses are related to the Papkovich-Neuber displacement potentials ϕ_0 and ϕ_1 as follows:

a) in Cartesian coordinates

$$2Gu_x = \frac{\partial \phi_0}{\partial x} + x \frac{\partial \phi_1}{\partial x} - \kappa \phi_1$$

$$2Gu_y = \frac{\partial \phi_0}{\partial y} + x \frac{\partial \phi_1}{\partial y} \qquad \text{(A1)}$$

$$\sigma_{xx} = \frac{\partial^2 \phi_0}{\partial x^2} + x \frac{\partial^2 \phi_1}{\partial x^2} - \frac{1}{2} (\kappa+1) \frac{\partial \phi_1}{\partial x}$$

$$\sigma_{yy} = \frac{\partial^2 \phi_0}{\partial y^2} + x \frac{\partial^2 \phi_1}{\partial y^2} - \frac{1}{2} (3-\kappa) \frac{\partial \phi_1}{\partial x}$$

$$\sigma_{xy} = \frac{\partial^2 \phi_0}{\partial x \partial y} + x \frac{\partial^2 \phi_1}{\partial x \partial y} - \frac{1}{2} (\kappa-1) \frac{\partial \phi_1}{\partial y}$$

b) in polar coordinates

$$2Gu_r = \frac{\partial \phi_0}{\partial r} + r \cos\theta \frac{\partial \phi_1}{\partial r} - \kappa \cos\theta \phi_1$$

$$2Gu_\theta = \frac{1}{r} \frac{\partial \phi_0}{\partial \theta} + \cos\theta \frac{\partial \phi_1}{\partial \theta} + \kappa \sin\theta \phi_1 \qquad \text{(A2)}$$

$$\sigma_{rr} = \frac{\partial^2 \phi_0}{\partial r^2} + r \cos\theta \frac{\partial^2 \phi_1}{\partial r^2} - \frac{1}{2} (\kappa+1) \cos\theta \frac{\partial \phi_1}{\partial r} + \frac{1}{2} (3-\kappa) \frac{\sin\theta}{r} \frac{\partial \phi_1}{\partial \theta}$$

$$\sigma_{\theta\theta} = \frac{1}{r}\frac{\partial\phi_0}{\partial r} + \frac{1}{r^2}\frac{\partial^2\phi_0}{\partial\theta^2} + \frac{\cos\theta}{r}\frac{\partial^2\phi_1}{\partial\theta^2} + \frac{1}{2}(\kappa-1)\cos\theta\frac{\partial\phi_1}{\partial r} + \frac{1}{2}(\kappa+1)\frac{\sin\theta}{r}\frac{\partial\phi_1}{\partial\theta}$$

$$\sigma_{r\theta} = \frac{1}{r}\frac{\partial^2\phi_0}{\partial r\partial\theta} - \frac{1}{r^2}\frac{\partial\phi_0}{\partial\theta} + \cos\theta\frac{\partial^2\phi_1}{\partial r\partial\theta} + \frac{1}{2}(\kappa-1)\sin\theta\frac{\partial\phi_1}{\partial r} - \frac{1}{2}(\kappa+1)\frac{\cos\theta}{r}\frac{\partial\phi_1}{\partial\theta}$$

where

$$\nabla^2\phi_1 = \nabla^2\phi_2 = 0$$

and

$$\nabla^2 = \frac{\partial^2}{\partial x^2} + \frac{\partial^2}{\partial y^2} = \frac{\partial^2}{\partial r^2} + \frac{1}{r}\frac{\partial}{\partial r} + \frac{1}{r^2}\frac{\partial^2}{\partial\theta^2}.$$